EXERGOECONOMIC ANALYSES OF A NOVEL SOLAR ORGANIC RANKINE CYCLE INTEGRATED WITH CASCADED VAPOR ABSORPTION-COMPRESSION REFRIGERATION SYSTEM

2024
MASTER THESIS
MECHANICAL ENGINEERING

Shawqi Hussein Krain AL-GAWWAM

Thesis Advisor
Assist. Prof. Dr. Abdulrazzak Ahmed Saleh AKROOT

EXERGOECONOMIC ANALYSES OF A NOVEL SOLAR ORGANIC RANKINE CYCLE INTEGRATED WITH CASCADED VAPOR ABSORPTION-COMPRESSION REFRIGERATION SYSTEM

Shawqi Hussein Karin AL-GAWWAM

Thesis Advisor
Assist. Prof. Dr. Abdulrazzak Ahmed Saleh AKROOT

T.C.
Karabuk University
Institute of Graduate Programs
Department of Mechanical Engineering
Master Thesis
Prepared as

KARABUK
April 2024

I certify that in my opinion the presented thesis that has been submitted by Shawqi Hussein Karin AL-GAWWAM titled "EXERGOECONOMIC ANALYSES OF A NOVEL SOLAR ORGANIC RANKINE CYCLE INTEGRATED WITH CASCADED VAPOR ABSORPTION-COMPRESSION REFRIGERATION SYSTEM" is fully adequate in scope and in quality as a thesis for the degree of Master of Science.

Assist. Prof. Dr. Abdulrazzak Ahmed Saleh AKROOT .....
Thesis Advisor, Department of Mechanical Engineering

This thesis is accepted by examining committee with the unanimous vote in the Dept. of Mechanical Engineering as Master of Science thesis. April 24, 2024.

Examining Committee Members (Institutions)		Signature
Chairman	: Prof. Dr. Emrah DENİZ (KBU)	.....
Member	: Prof. Dr. Ali Etem GÜREL (DU)	.....
Member	: Assist. Prof. Dr. Abdulrazzak AKROOT (KBU)	.....

The degree of Master of Science by the thesis that has been submitted was approved by the Administrative Board of Institute of Graduate Programs, Karabuk University.

Assoc. Prof. Dr. Zeynep ÖZCAN .....
Director of the Institute of Graduate Program

"I declare that all the information that has been presented in this thesis was gathered and presented in accordance with ethical principles and academic regulations and I have according to requirements of those regulations and principles that were cited all those which don't originate in this work too."

Shawqi Hussein Krain AL-GAWWAM

ABSTRACT

Master Thesis

EXERGOECONOMIC ANALYSES OF A NOVEL SOLAR ORGANIC RANKINE CYCLE İNTEGRATED WITH CASCADED VAPOR ABSORPTION-COMPRESSION REFRIGERATION SYSTEM

Shawqi Hussein Krain AL-GAWWAM

Karabük University
Institute of Graduate Programs
Department of Mechanical Engineering

Thesis Advisor:
Assist. Prof. Dr. Abdulrazzak Ahmed Saleh AKROOT
April 2024,74 pages

This research proposes a model for a solar combined cooling heating power (SCCHP) system that combines cooling, heating, and electricity generation. The system is precisely engineered to cater to the needs of government institutions, large-scale hospitals, and residential complexes located in Baghdad, Iraq. The system undergoes a 3E investigation, examining energy, exergy, and exergoeconomic aspects. The SCCHP system generates 210 kW of electricity, 3965 kW of heat, and has a cooling load of 249.4 kW. The system's energy efficiency was calculated to be 76.55%, while its exergy efficiency was judged to be 17.75%. The exergoeconomic factor of the SCCHP system was calculated as 63.32%, showing that the fraction of costs associated with exergy destruction is lower than the initial capital investment cost of the system. The exergoeconomic importance of the solar power tower collectors (SPTC) and ORC evaporator is most significant. An investigation is

conducted into the impact of ORC working fluid change and ORT inlet temperature. Octane is more efficient from a work net and exergoeconomic standpoint, while R245fa is more efficient from an energy and exergy standpoint. Increasing the ORT inlet temperature reduces the work net, increases the total cost rate, and diminishes the thermal and exergy efficiencies of the system.

Key Word **:** SCCHP system, Exergoeconomic, Cascade refrigeration system, ORC, SPTC, Combined heat, and power (CHP)

Science Code: 91436

ÖZET

Yüksek Lisans Tezi

KADEMELİ BUHAR SOĞURMA-SIKIŞTIRMA SOĞUTMA SİSTEMİ İLE ENTEGRE YENİ BİR GÜNEŞ ENERJİLİ ORGANİK RANKİN ÇEVRİMİNİN EKONOMİK ANALİZİ

Shawqi Hussein Krain AL-GAWWAM

Karabük Üniversitesi
Lisansüstü Eğitim Enstitüsü
Makine Mühendisliği Anabilim Dalı

Tez Danışmanı:
Dr. Öğr. Üyesi Abdulrazzak Ahmed Saleh AKROOT
Nisan 2024, 74 sayfa

Bu araştırma, soğutma, ısıtma ve elektrik üretimini birleştiren bir güneş enerjili birleşik soğutma ısıtma gücü (SCCHP) sistemi için bir model önermektedir. Sistem, Bağdat, Irak'ta bulunan devlet kurumları, büyük ölçekli hastaneler ve konut komplekslerinin ihtiyaçlarını karşılamak için hassas bir şekilde tasarlanmıştır. Sistem enerji, ekserji ve eksergoekonomik açılardan incelenerek 3E araştırmasına tabi tutulmuştur. SCCHP sistemi 210 kW elektrik, 3965 kW ısı üretmekte ve 249,4 kW soğutma yüküne sahiptir. Sistemin enerji verimliliği %76,55 olarak hesaplanırken, ekserji verimliliği %17,75 olarak değerlendirilmiştir. SCCHP sisteminin ekserjoekonomik faktörü %63,32 olarak hesaplanmıştır, bu da ekserji yıkımı ile ilişkili maliyetlerin sistemin ilk sermaye yatırım maliyetinden daha düşük olduğunu göstermektedir. Güneş enerjisi kule kolektörlerinin (SPTC) ve ORC buharlaştırıcının

ekserjoekonomik önemi en büyüktür. ORC çalışma sıvısı değişimi ve ORT giriş sıcaklığının etkisi üzerine bir araştırma yapılmıştır.

Oktan, iş ağı ve ekserjoekonomik açıdan daha verimliyken, R245fa enerji ve ekserji açısından daha verimlidir. ORT giriş sıcaklığının artırılması net işi azaltmakta, toplam maliyet oranını artırmakta ve sistemin termal ve ekserji verimliliğini azaltmaktadır

Anahtar Sözcükler : SCCHP sistemi, ekserjoekonomi, Ardışık soğutma sistemi, ORC, SPTC, birleşik ısı ve güç (CHP)

Bilim Kodu : 91436

ACKNOWLEDGMENT

Praise be to God, Lord of the Worlds, and prayers and peace be upon the Seal of the Prophets and Messengers, our Master Muhammad, may God bless him and grant him peace, and upon all his family and companions. Oh God, all praise and thanks be to You for the best of Your gifts, O possessor of knowledge, from You we learn and from You we seek help and in Your blessings we rely, for You are the best protector and the best of doers.

First of all, I ask God Almighty that I have succeeded in preparing this message, and I am happy to dedicate this humble work to the one who raised me when I was young, inspired me with knowledge, patience, and goodness, and included me in the garden of his tenderness (my dear father and mother). May God protect them and honor them with goodness. They are the support and light of the heart and eyes.

To those who helped me and supported me throughout my studies and contributed to the completion of my study project and the completion of my master's thesis, my dear wife, my beloved children, and my dear children.

I would also like to dedicate my thanks, appreciation, and effort to Assist. Prof. Dr. Abdulrazzak AKROOT for his effort and credit in guiding me.

My continued thanks to the administration of the Department of Mechanical Engineering at Karabük University and its distinguished staff, especially the head of the department Prof.Dr. Emrah DENİZ I am thankful for their efforts in obtaining the certificate.

I also dedicate this achievement to my dear country, Iraq, to my beloved city of Baghdad, which is steadfast in its people, and to the country that hosted me throughout my studies, Turkey.

CONTENTS

Page

Page

LIST OF FIGURES

Page

Page

LIST OF TABLES

Page

SYMBOLS AND ABBREVITIONS INDEX

SYMBOLS

A_coll	: collector area (m2)
C	: exergy cost per unit ($/GJ)
COP	: coefficient of performance
C	:cost Rate ($/hr)
DNI	: direct normal irradiations (W/m2)
E	:energy (kW)
(EX)	:exergy flows (kW)
F	:exergoeconomic factor (%)
h	:specific enthalpy (kJ/kg)
m	:mass flow rate (kg/s)
n	:system life time
P	:pressure (kPa)
Q	:heat transfer (kW)
s	:specific entropy (kJ/kg. K)
T	:temperature (°C)
U	:overall heat transfer coefficient (W/m2.K)
W	:work done (kW)
Z	:initial cost rate ($/hr)

Greek symbols

ŋ	:efficiency (%)
τ	:operation hour (h)
φ	:maintenance factor
ψ	:exergy efficiency (%)

Subscripts

Abs	:absorber
Col	:collector

Comp :compressor

Condcondenser

EV :expansion valve

Evap :Evaporator

Gen :generator

SHES :sensible heat exchanger

SR :solar reservoir

t :Tank

Abbreviations

ARC :absorption refrigeration cycle

HE :heat exchanger

HRSG :heat recovery steam generation

HTF :heat transfer fluid

ORC :organic Rankine cycle

ORT :organic Rankine turbine

P :pump

RES :renewable energy sources

SCCHP :solar combined cooling heating power

SE :solar energy

SPTC :solar power tower collectors

TST :thermal storage tank

VARS :vapor absorption refrigeration system

VCRS :vapor compression refrigeration system

CHAPTER 1

INTRODUCTION

Sustainable energy development aims to lessen environmental impacts while boosting energy efficiency to economically supply the growing energy demand. There was a widespread belief that combined cooling, heating, and power (CCHP) systems could be a practical way to address the diverse energy demands due to the unique characteristics of cascade energy applications. These applications generate electricity from a primary source and helpful heat and cooling through heat recovery and utilization systems powered by waste heat [1].

The sharp decline of fossil resources like coal and oil has caused an energy crisis that countries worldwide are trying to cope with it. The importance of the "carbon neutrality" strategy is growing as air pollution and carbon dioxide emissions worsen. Because of this, research into alternatives to traditional energy sources, such as solar power, has been a growing area of focus for scientists [2].

Clean, highly efficient methods of energy conversion and usage are critically required in light of the worldwide energy crisis and environmental contamination. A possible solution to energy and environmental challenges could be the CCHP (Combined Cooling, Heating, and electricity) system, which is an efficient, clean, dependable, versatile, and cost-effective way to generate electricity, heat, and cooling all at once [3].

Solar-powered combined heating and cooling power (SCCHP) systems use waste heat from primary sources while also utilizing clean and renewable resources to boost efficiency, lower costs, and minimize pollutant generation, making them viable options for cleaner manufacturing. [4].

The SCCHP system is renowned for its minimal maintenance needs and extended operational longevity. The system integrates solar thermal energy, absorption refrigeration, and cogeneration, focusing on long-term durability and reliability. This durability ensures a steady provision of energy and enhances the system's cost-effectiveness by minimizing the requirement for frequent repairs or replacements.

1.1. BACKGROUND INFORMATION

Solar energy is becoming increasingly integrated and pervasive due to continuously improving combined cooling, heating, and power (CCHP) technology in response to increasing concerns about energy sustainability. When coupled with a combined heat and power (CHP) system, solar technologies can displace inefficient older systems by transforming solar radiation into usable thermal and electrical energy [5].

Solar thermal technology can raise the temperature of a gas or liquid by absorbing solar radiation; this makes it useful for various applications, including heating, cooling, and power generation. Despite the technology's longevity, it has only gained traction due to its potential to lessen reliance on fossil fuels [6,7].

The efficient process of cogeneration generates both electrical power and thermal energy simultaneously. The technology drastically reduces energy waste by producing heat and electricity from the same fuel source [8].

Compared to older vapor compression refrigeration systems, absorption refrigeration uses less energy because it uses heat to cool. It's the perfect cooling solution for hotter areas when combined with solar thermal technology. [9].

The CCHP system is a result of combining these technologies; it is both an efficient and environmentally beneficial energy system. Carbon emissions are decreased by using renewable energy sources to generate power, heat, and cool the building. This is illustrated in Figure 1.1 [10]. If implemented, this technology might radically alter the energy sector, leading to a brighter, more sustainable future for all people [11]. With the continuous progress of technology, experts can anticipate the development

of highly efficient and economically viable combined cooling, heating, and power (CCHP) systems shortly. Therefore, the global community must persist in researching and allocating resources toward developing these technologies to fulfill our escalating energy demands while minimizing environmental damage. By incorporating Combined Cooling, Heating, and Power (CCHP) systems and other environmentally friendly energy solutions, the researchers may actively contribute to creating a more sustainable planet for future generations. They contribute to advancing and endorsing combined cooling, heating, and power-generating systems to foster a more improved and environmentally friendly future.

Denklem 1

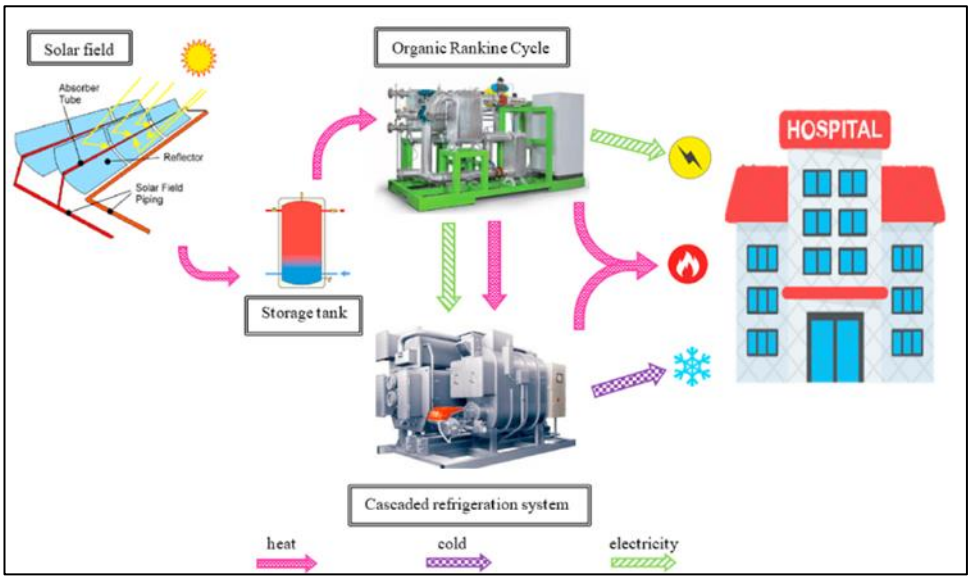

Figure 1.1. Schematic diagram of the CCHP system [12].

The amalgamation of these three technologies provides several benefits [13,14]:

- Minimized Carbon Emissions: By using renewable solar energy and reducing fossil fuel consumption, this system can substantially decrease carbon emissions, making a valuable contribution towards a cleaner environment.
- Cost Efficiency: Users can obtain long-term cost savings by utilizing solar energy and limiting reliance on additional fuel sources.

- Versatility: This system is capable of providing both cooling and heating functions, making it well-suited for a wide range of residential and industrial uses.
- Reliability: Integrating multiple technologies into a unified system ensures a reliable energy source, which protects against power outages and disturbances.
- Energy Efficiency: the absorption chiller can work more efficiently by utilizing the waste heat from the cogeneration unit, which results in substantial energy conservation.

1.2. SOLAR ENERGY (SE)

Solar energy is a form of renewable energy derived from the sun. It is a highly clean and plentiful energy source on Earth. The utilization of sunshine as an energy source has been present since ancient times, with the Greeks and Romans employing solar power to warm their residences. Nevertheless, it was during the 20th century when solar panels were invented and employed for commercial purposes [15,16].

The supply of SE is continuously refreshed and will never be exhausted. Solar electricity is extremely sustainable and has a negligible environmental footprint. It is completely devoid of any greenhouse emissions and has an extremely small ecological impact. This makes it an essential tool in the fight against climate change and the reduction of our carbon emissions [17,18].

Solar energy has a wide range of uses, including powering residential buildings and supplying electricity to rural regions. Common applications of solar energy include [19,20]:

- Producing electricity for homes and businesses
- Transporting water in rural or isolated regions
- Warming water for household purposes or recreational swimming pools.
- Supplying energy for lamps and traffic signals.
- Generating power for satellites and spacecraft in outer space.

- Supplying electricity to remote areas without access to the power grid or areas affected by disasters.

Furthermore, solar energy has been utilized for the purposes of cooking, desalinating water, and propelling autos. With the progression of technology, the range of possible applications for solar energy is always growing.

1.3. SOLAR THERMAL SYSTEM

Solar thermal systems utilize sunlight to heat water or air directly instead of turning it into electrical energy. Typically, these systems employ mirrors to focus sunlight onto a receiver, heating a fluid to produce steam and drive a turbine.[21,22] . This method is frequently employed in solar power plants of significant scale. Utilizing solar energy systems offers numerous advantages, such as [23,24]:

- Sustainable: Solar energy is a sustainable energy source, as the sun's rays continuously replenish it and will not be depleted as long as the sun is active.
- Can be used in remote areas: Solar energy systems are suitable for installation in isolated places that lack access to the main power grid, thereby enabling the provision of electricity to individuals who would otherwise be without it.
- Economical: Solar energy systems can yield long-term savings by reducing electricity expenses despite the high upfront price.
- Environmentally friendly: Unlike fossil fuels, solar energy does not emit detrimental environmental pollutants. This implies that it aids in the reduction of air pollution and the mitigation of climate change.
- Minimal upkeep: Solar energy systems necessitate very little maintenance, as most manufacturers provide warranties of up to 25 years for their goods.

1.4. ORGANIC RANKINE CYCLE

The organic Rankine cycle (ORC) is a thermodynamic cycle that uses organic fluids as the working medium. It operates similarly to the standard steam Rankine cycle but replaces water with organic fluids for increased efficiency in a closed-loop system

[25]. During the 1950s, an experimental group led by Professor Szeftel at the University of Paris devised the Organic Rankine Cycle (ORC). After its inception, the ORC has become a viable alternative for generating electricity, particularly well-suited for harnessing low-temperature heat sources [26,27].

The ability of an ORC system to utilize low-grade heat sources unsuitable for conventional steam power plants is one of its primary advantages [28]. Utilizing residual heat to generate electricity is thus an exceptionally efficient and economical method. Moreover, compared to water, organic fluids have a higher vapor density, resulting in diminished apparatus dimensions and reduced installation costs. In contrast to power-generating systems that depend on fossil fuels, the ORC system demonstrates reduced emissions, constituting a more ecologically sustainable substitute.

Also, it is possible to seamlessly integrate the ORC system with additional renewable energy sources, including solar or biomass, to create a hybrid power plant. This facilitates continuous electricity production, even when a single source is unavailable.

1.5. SOLAR-ASSISTED ORGANIC RANKINE CYCLE

As depicted in Figure 1.2 [29], the Solar-assisted Organic Rankine cycle (SORC) is a power generation system that employs solar energy (SE) to propel an ORC and generate electrical output. The ORC technology is gaining popularity as it offers a renewable and environmentally friendly alternative for electricity generation.

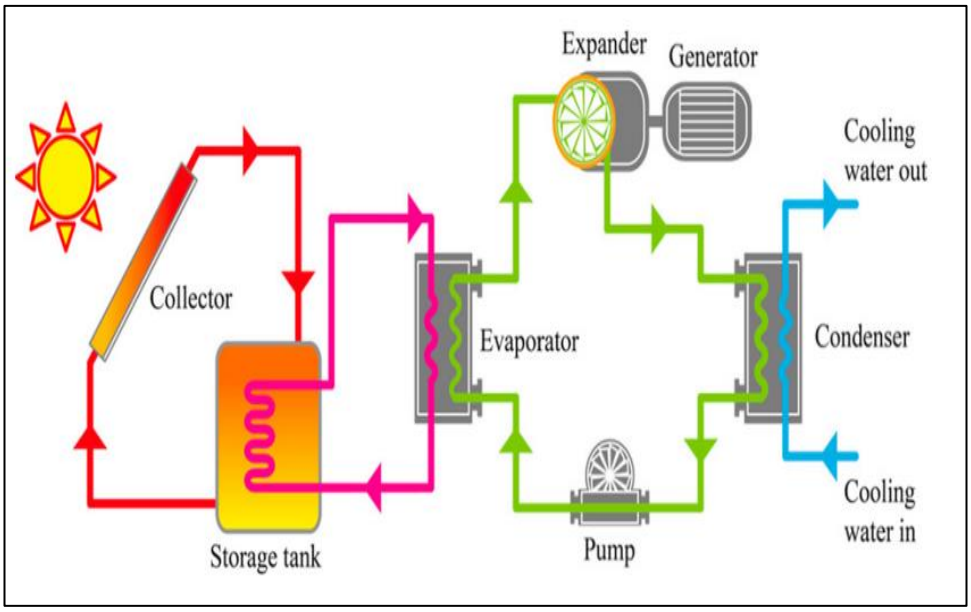

Figure 1.2. Schematic diagram of a solar ORC system [30]

The SORC's outstanding performance in low temperatures makes it an ideal choice for areas with limited sun exposure. Because of these capabilities, it is an appealing choice for remote and rural locations that do not have access to traditional power systems. Moreover, the use of organic working fluids enhances the environmental sustainability of the system, as these substances are chosen for their negligible effect on ozone depletion and limited potential for contributing to global warming.

SORC technology is applicable to an extensive variety of applications, including [31,32]:

SORC technology is applicable to an extensive variety of applications, including SORC technology can be applied to a wide range of applications, including [23,24]:

- Integrating the SORC system with industrial processes allows for the capture and conversion of residual heat into electricity, hence enhancing overall energy efficiency.
- The SORC system has the ability to generate electricity for industrial, commercial, and residential purposes.

- The SORC system has the ability to generate power while simultaneously purifying brackish or saltwater sources.
- SORC systems have the ability to use the waste heat generated by the ORC cycle to either heat or cool areas.
- The primary goal of integrating SORC systems is to produce electricity and meet the power needs of residential, commercial, and industrial settings.
- Researchers are currently studying the possibility of using SORC technology in hybrid vehicles within the automotive industry. This technology serves two main purposes: enhancing electricity generation and improving fuel economy.

While SORC technology offers considerable benefits, certain obstacles must be surmounted before its extensive implementation:

- Meticulous design considerations are necessary for optimal performance when integrating the ORC system with auxiliary technologies like thermal storage and heat exchangers.
- The initial implementation of the system may involve significant expenses, which could make it less appealing for some applications. However, prices are expected to decrease due to technological advancements and the advantages of increasing manufacturing scale.
- The choice of materials and working fluid may impact the system's durability and reliability. It is imperative to meticulously select materials compatible with the working fluid to guarantee long-term functionality.
- The ORC system's flexibility is affected by solar irradiation and ambient temperature variations. Therefore, it is necessary to carefully examine the system to improve its effectiveness in various operational situations.

Despite these challenges, ongoing efforts are being made to progress and improve solar-assisted ORC systems. Potential developments in this domain comprise [33,34]:

- To achieve extensive implementation, it is critical to surmount financial obstacles; continuous endeavors are underway to diminish the costs linked to solar-assisted ORC systems.
- By integrating solar-assisted ORC with renewable energy sources such as wind or geothermal, the efficiency and dependability of the system can be improved.
- Improving the performance of the Organic Rankine Cycle (ORC) system's performance requires developing novel heat transfer fluids and implementing inventive control strategies to ensure greater efficiency in the face of fluctuating conditions.
- Although laboratory experiments have shown promise, additional research, and practical implementations are required to validate their viability on a larger magnitude.

1.6. CASCADE ABSORPTION-COMPRESSION REFRIGERATION SYSTEM

A cascade absorption-compression refrigeration system is a sophisticated refrigeration technology that integrates the principles of absorption and compression cycles. This is illustrated in Figure 3.1 [35]. This technology is employed when conventional single-stage vapor compression systems are inadequate for cooling large-scale commercial and industrial applications [36].

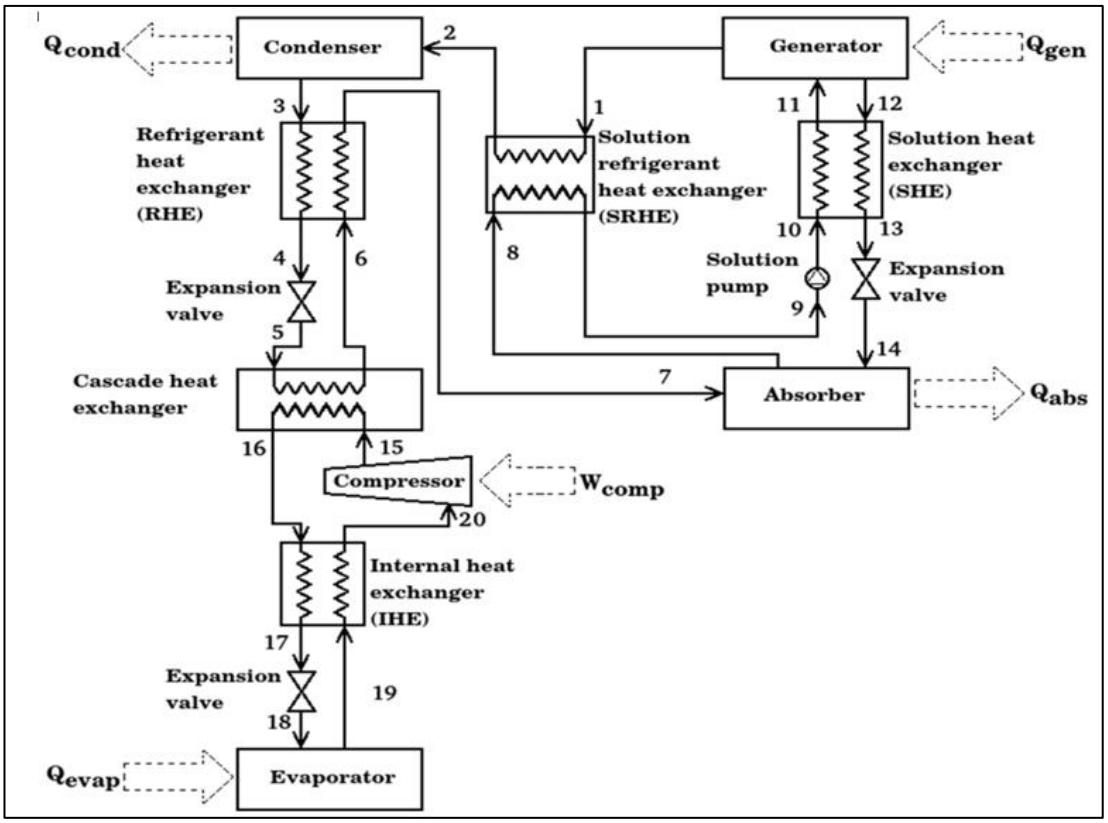

Figure 1.3. Schematic illustration of the compression-absorption hybrid system [37].

The cascade absorption-compression refrigeration system technology offers several noteworthy advantages, which are outlined below [38]:

- The absorption cycle operates at reduced pressure and temperature levels, exhibiting a broad range. As a result, it is highly suitable for tasks requiring decreasing temperatures. On the other hand, applications necessitating moderate to high temperatures can effectively utilize the vapor compression cycle due to its ability to withstand elevated temperatures.
- The implementation of two separate circuits leads to a reduction in the charge of the refrigerant, which in turn mitigates the environmental impacts and costs associated with refrigerants.
- The cascade configuration facilitates enhanced utilization of both refrigerant circuits, resulting in a higher coefficient of performance (COP) than vapor compression systems with a single stage. This leads to a significant increase in efficacy.

- The inclusion of two separate circuits affords an increased level of adaptability in the system design process. This feature facilitates increased accuracy in regulating operational parameters and permits tailoring to accommodate specific cooling requirements.
- The absorption cycle is highly compatible with waste heat recovery because it efficiently converts low-grade waste heat into usable energy. Consequently, it is an environmentally preferable substitute for traditional refrigeration systems.

Continuous research and development endeavors in refrigeration systems are focused on improving operational effectiveness, mitigating ecological impacts, and expanding application domains. The following are potential future developments in cascade absorption-compression refrigeration systems[39]:

- Utilizing renewable energy sources such as solar, geothermal, or industrial residual heat to power the absorption cycle.
- The implementation of intelligent control systems involves the use of advanced control algorithms and sensors to maximize the performance of refrigeration systems and reduce energy consumption.
- Miniaturization involves the development of smaller and more compact systems that are suitable for domestic or small-scale applications.
- Ongoing research aims to develop sustainable alternatives to address concerns regarding the environmental impact and safety of conventional refrigerants utilized in cascade absorption-compression systems.

1.7. THERMAL ENERGY STORAGE SYSTEMS

Thermal energy storage systems are designed to store thermal energy in a specific medium, enabling later utilization. These systems are crucial in multiple industries, such as power generation, industrial operations, and building heating and cooling. They facilitate the reduction of reliance on fossil fuels by enabling the storage of renewable energy sources for future utilization while aiding in the equilibrium of energy supply and demand [40].

Thermal energy storage systems have a wide range of applications, including [41]:

- Solar thermal power plants can store thermal energy during the day and convert it into electricity at night, enabling uninterrupted operation of the power plant.
- Thermal energy storage can be employed in industrial processes, including food processing, cement manufacture, and chemical manufacturing, to mitigate the reliance on fossil fuels and decrease emissions.
- Thermal energy storage can be integrated into district heating systems to store surplus heat produced during low-demand hours for use during high-demand periods.
- Thermal energy storage in buildings can decrease the highest level of demand for heating or cooling, leading to financial savings and improved effectiveness.
- Electric vehicles can benefit from thermal energy storage, which enhances the efficiency and range of the cars by serving as a heating or cooling source for the battery system.

1.8. THESIS MOTIVATION

The energy needs of Iraq are predominantly met by the utilization of fossil fuels, specifically oil and natural gas, which contribute to around 90% of its electricity production. Excessive reliance on non-renewable sources exhausts the nation's natural resources and substantially impacts air pollution and the release of greenhouse gases. The release of harmful pollutants into the atmosphere due to the combustion of fossil fuels has negative consequences for human health and contributes to climate change.

Iraq is subjected to severe heat, experiencing summertime temperatures that reach unbearable heights of 50 degrees Celsius. This extreme weather makes daily life challenging, particularly in cities where air pollution and overcrowding exacerbate the oppressive heat. During the hot season, the increasing demand for air

conditioning in Iraq strains the country's already inadequate electricity infrastructure, resulting in frequent blackouts and load shedding.

This thesis investigates applying solar-powered Combined Cooling, Heating, and Power (SCCHP) systems in Baghdad, Iraq, with the dual objectives of reducing carbon emissions and fulfilling the nation's energy requirements sustainably. SCCHP systems, which harness solar energy for ventilation, heating, and electricity using solar collectors, provide dependable power even during an outage, long-term cost savings, and minimal upkeep requirements.

1.9. THESIS OBJECTIVE

The main objectives of the proposed system are enumerated as:

- To propose implementing a Solar Combined Cooling, Heating, and Power (SCCHP) system to effectively meet the energy requirements of prominent medical facilities, government structures, and residential complexes in Baghdad, Iraq.
- To assess the exergoeconomic significance of individual components within the SCCHP system.
- To examine the influence of critical operational variables on the efficiency of the SCCHP system. Specifically, it will analyze the consequences of modifying the working fluid and inlet temperature of the Organic Rankine Turbine (ORC and ORT, respectively).

1.10. THESIS STRUCTURE

The thesis is organized into five chapters. The first chapter comprehensively introduces the Solar Combined Cooling Heating Power (SCCHP) system, including thorough insights into its subsystems, research objectives, and rationale. The second chapter includes a comprehensive examination of the existing literature relevant to the SCCHP system. The third chapter provides a comprehensive account of the examined SCCHP system, thoroughly explaining its operational principles and the

balancing equations for mass, energy, exergy, and cost for each system component. The fourth chapter examines and contrasts the simulation outcomes of the suggested model with the discoveries of prior investigations. Ultimately, the fifth chapter succinctly presents the study's findings derived from the research results.

CHAPTER 2

LITERATURE REVIEW

Solar-assisted systems have become a crucial pathway in sustainable energy solutions, providing a versatile strategy to meet the increasing cooling, heating, and power production needs. As the world strives to shift towards cleaner and sustainable energy sources, incorporating solar technologies emerges as a symbol of hope. This chapter investigates the current understanding of solar-assisted systems, analyzing their technological development, performance attributes, and usage within the broader sustainable energy framework.

Hou et al. [42] examined a Guangzhou residential complex's SCCHP system. The study examined the system's architecture and optimal performance. The solid oxide fuel cell (SOFC) generates power in the SCCHP system. Electric and absorption chillers, heat storage tanks, photovoltaic systems, solar ETCs, and heat recovery systems are all included. The SCCHP system was assessed for cost, primary energy use, and emissions. Integration criteria and optimization methods like Particle Swarm Optimization (PSO) improved feasibility assessment. Despite saving 15,141.63 kilowatt-hours, the updated SCCHP system produced 170,183.57 megajoules of yearly heat. With 11.2 years of amortization, the investment returned 2.55.

An integrated CCHP system powered by renewable energy sources (RES) was shown by Zhang et al. [43], using biogas-fueled ICE and PV panels. This RES-CCHP system was tested on a Jinan, China, farm, unlike the usual natural gas CCHP system. Direct energy savings of 20.94% were achieved with the optimized design. Cost savings of 11.73% annually. RES-CCHP reduced carbon emissions by 40.79% over typical systems. This study shows how RES-CCHP systems can promote sustainable energy and reduce environmental impact.

Chain et al. [44] developed a solar-assisted combined cooling and power system (SCCP) that efficiently uses waste heat and renewable energy sources to provide electricity and cooling to a cold storage facility. The SCCP system consists of an internal combustion engine, thermal storage, a combined power and refrigeration system that uses ammonia and water, and evacuated tube collectors. Energy and energy are critical factors for assessing system efficiency. The study also evaluates the best system architecture and the impact of essential components. Quantitative analyses show that the SCCP system has a renewable energy ratio of 18.1% and a thermal efficiency of 70.35%. Furthermore, the system's exergy efficiency is calculated to be 45.52%. Notably, the coefficient of exergy destruction is critical in comprehending the system's energy-saving mechanism and future development potential. The study examines the effects of essential parameters such as turbine input and generation pressure by analyzing condensation and absorption temperatures. The final goal is to determine the most efficient configuration for the system.

Ravindra and Ramgopal [45] compared two solar-assisted combined heat and power systems. One method used an expansion turbine, while the other used a throttle valve. The researchers created a thermodynamic model to evaluate the efficiency of a solar-powered CCHP system under stable operating conditions and study the essential thermodynamic parameters and their impact on system performance. Notably, the design with the expansion turbine resulted in higher cooling user output and enhanced electrical power production. Careful selection and design of system components can reduce exergy losses while increasing energy usage efficiency. Improving the isentropic efficiency of the CO_2 compressor and adjusting the recovery heat exchanger can increase exergy efficiency.

Salimi et al. [46] examined CCHP systems at hospitals, airports, desalination plants, wastewater treatment plants, and hydrogen production sites. Their main goal was to use renewable energy to reduce energy use and environmental impact. Optimizing CCHP system components like the combustion engine can boost efficiency and reduce carbon and water footprints. These systems use renewable energy instead of

fossil fuels, reducing carbon emissions. Solar hybrid systems can also reduce carbon and water footprints in areas with ample radiation.

Tonekaboni et al. [47] explored how porous media and nanofluids in solar collectors could improve SCCHP system efficiency. The study found that solar collectors using copper porous media (95% porosity) and nanofluids (CuO and Al2O3) improved energy and exergy efficiency by calculating the correct concentration to prevent sedimentation. The most significant efficiency improvement occurred at 0.5% nanofluid. However, adding 0.6% nanofluid to parabolic collectors with copper porous materials caused sedimentation and increased pipe pressure, lowering energy efficiency.

Wang and Fu [48] created an Organic Rankine Cycle-based solar-assisted combination cooling, heating, and power (SCCHP) system. Dimethyl ether powers the primary mover and auxiliary boiler. Under typical summer and winter conditions, thermodynamic and economic approaches analyzed the system's performance. The proposed system showed that the Follow Electric Load (FEL) method may meet considerable energy demand while reducing carbon dioxide emissions. The study found that SCCHP-ORC is 9.87% more efficient than the original system. It might significantly reduce winter and summer carbon dioxide emissions.

Assareh et al. [49] studied a solar-geothermal CCHP system with a hydrogen component. The system integrated photovoltaic/thermal collectors, steam turbines, a fuel cell circuit, a heat pump, an absorption chiller, and hydrogen and electricity storage units. Transient evaluation and the Response Surface Method (RSM) assessed its energy and economic performance. A Design of Experiments (DOE) technique optimized the system configuration to improve efficiency, minimize life cycle costs, and lower power and natural gas usage. Hydrogen storage and batteries improved component performance by 90% for the electrolyzer, 60% for the fuel cell, 23% for the PV/T solar collector, and 18% for the electrical generator annually. Research showed that the SG-CCHP system reduced thermal comfort scores, total power usage, and annual lifespan costs, demonstrating its energy-efficient and sustainable design potential.

Heydari and Sadati [50] explored how different materials used to create the office building envelope affected the effectiveness and efficiency of a CCHP (Combined Cooling, Heating, and Power) system. The researchers replicated a prototype office structure in Semnan, Iran, and calculated thermal demands for several building envelope designs. They then created a hybrid SCCHP (Solar Combined Cooling, Heating, and Power) system based on the load data from each scenario. The key findings demonstrated that improving window arrangement and insulating walls and roofs could result in a significant 24.8% reduction in peak generation unit (PGU) capacity and a substantial 53.48% drop in fuel consumption within the CCHP system. The study also looked into ways to enhance the building envelope to reduce energy waste and harness solar energy using a photovoltaic system.

Wang et al. [51] proposed a SCCHP system that incorporates a solar thermal collector, an internal combustion engine, a heat exchanger, an absorption heat pump, and a thermal storage tank. They applied an investigation of the energy, exergy, exergo-environmental, and exergo-economic performances of the hybrid system through thermodynamic modeling and validation. The studies assessed the effects of supplementation under static design settings and thermal storage on system efficiency and product unit costs. The hybrid system has shown a capacity to save 11.3% of natural gas, diminish carbon dioxide emissions, and decrease the time it takes to recover the initial investment by 1 year when compared to typical CCHP systems that do not use solar energy. The solar-assisted hybrid CCHP system attains an annual exergy efficiency of 22.4% and an energy efficiency of 76.3%. The hybrid system decreases carbon dioxide emissions, achieves an 11.3% reduction in natural gas consumption, and accelerates the capital payback time by 1 year compared to typical CCHP systems that do not use solar energy.

Han et al. [52] introduced a new solar-assisted methanol CCHP system that enhances the system's overall performance. The researchers proposed an optimization model with multiple objectives that consider exergo-economics. This model employs cost allocation based on energy levels to enhance the system's efficiency, economics, and environmental impact. Primary energy consumption, total product unit exergy cost, carbon dioxide emissions, collected solar energy, and yearly energy and exergy

efficiencies were among the many areas that saw substantial improvements. The total commodity unit exergy cost rose 49.0% compared to the reference system. However, primary energy usage dropped 22.6%, and carbon dioxide emissions dropped 70.6%. The system improved 15.9% in annual energy efficiency and 17.3% in exergy efficiency. The amount of solar energy collected increased by 37.6%. The sensitivity analysis demonstrated that primary energy use, carbon dioxide emissions, supplemental heat/heat storage ratios, and total product unit exergy cost are all connected.

Wang et al. [53] optimized a solar-natural gas hybrid combined heat and power (CCHP) system. The suggested arrangement includes solar PV panels, a flat-plate heat collector, and an integrated CCHP system. It also uses thermodynamic analysis to optimize the CCHP system and build energy supply and demand matching. Energy and exergy efficiencies dominated the thermodynamic performance evaluations of PV panels and heat collectors. Performance-affecting factors included electric load factor, installation ratio, solar irradiation, and load. CCHP systems with solar PV technology increase exergy efficiency. Installing a solar heat collector boosts energy efficiency.

Wang et al. [54] used concentrated photovoltaic/thermal (PV/T) solar collectors to maximize solar energy utilization and reduce greenhouse gas emissions in a natural gas CCHP system; They proposed optimizing the PV coverage ratio on the PV/T collector to minimize hybrid CCHP system expenses. After incorporating and refining PV/T technology, system items are 6.4% cheaper. The results show that the 1.0 coverage ratio reduces system product costs. This reduced system items' specific costs by 6.4%. Compared to conventional exergo-economic study, exergy-analysis-based particular system cost power was 20.3% higher. However, heat exergy costs fell. The hybrid CCHP system's PV/T collectors were integrated and optimized to maximize solar energy utilization and reduce greenhouse gas emissions.

A multi-mode solar-assisted absorption-compression system (SAACS) powered by solar heat and electricity was studied by Chen et al. [55] for household cooling, heating, and annual domestic hot water production. Integrating the absorption

subsystem (ABS) with a vapor compression subsystem (VCS) raises the evaporator temperature to prevent freezing. Due to lower target-producing temperatures, the ABS could heat and cool in winter and summer. SAACS utilized solar heat to create power annually, improving solar collector efficiency per unit area, cost-effectiveness, and stability compared to 100% solar heating-cooling systems. The study showed that VCS-ABS hybrid cooling and heating systems are economically viable and efficient.

A novel system that uses solar thermal energy for heating and cooling is the sun-assisted absorption-compression system introduced by Chen et al. [56]. This research compared the efficiency of the proposed system to that of air-source heat pumps operating in identical environmental settings. The use of performance metrics like power-saving ratio (PSR), COP ele increase, and energy-saving ratio (ESR) allows for the evaluation of the proposed system's performance. The solar collection efficiency was enhanced by integrating the vapor compression subsystem with the absorption heat pump, which reduced heat-generated temperature. At 80°C, the hot water temperature achieves the maximum increase in PSR and COP ele in solar-assisted heating mode, with values of 31.4% and 45.8%, respectively. The statistics for solar-assisted cooling mode are 16.0%, and for traditional cooling mode, 18.9%. Because of the many coupling mechanisms at work, the speed of the terminal and compressor fans has a more significant impact on heating performance than cooling performance.

Tan et al. [57] assessed the performance of a novel CCP/CHP system that integrates a modified SOFC-GT plant with a solar-assisted LiBr absorption cooling/heating unit. The system successfully achieved equilibrium in both power generation and cooling/heating production, while also integrating renewable energy sources inside the microgrid. The heat extracted from the plant exhaust and the solar hot water attained optimal thermal compatibility in the suggested double-effect LiBr absorption cycle.

Su et al. [58] proposed a new CCHP system based on biogas steam reforming for application, which improved integrated performances and reduced the payback

period by 49.5% compared to conventional systems. The study emphasized the capacity of solar energy in CCHP systems, which can transform SE into several outputs, such as cooling, power, and heat, by using syngas inside a traditional CCHP. This technique minimized irreparable losses in directly burning biogas and achieved the sequential exploitation of solar energy, thus enhancing the system's efficiency. The experimental and computational findings demonstrate that the methane conversion rate in the biogas steam reforming reaction exhibits an increase from 80.85% to 99.94% with the elevation of the reaction temperature from 650°C to 900°CThe experimental data demonstrate a close correspondence with the simulation results for CO2 conversion rates between 650°C and 700°C. However, the experimental results indicate lower CO2 conversion rates than the simulation results for temperatures over 750°C.

Wang and Yang [59] suggested a hybrid CCHP system that utilizes both solar energy and biomass as energy sources. They examined how these two sources complement each other to improve the system's overall energy efficiency. An analysis was conducted on the performances of the CCHP system under various operating situations. The method for enhancing energy efficiency was examined based on the system's thermodynamic performance, which included primary energy ratios and exergy efficiencies at different energy proportions. This study investigated the thermodynamic performances of the CCHP system under variable external conditions and energy ratios. The primary energy ratio was 57.9%, and the exergy efficiency was 16.1% at the design condition. Additionally, the carbon emission reduction ratio was approximately 95.7%.

Bahria et al. [60] devised a parametric optimization technique using dynamic simulation to examine solar thermal systems for space heating, hot water, and cooling. They Compared two construction types: typical construction in Algeria (low thermal mass, single glazing) and a high-energy-performance building (double glazing) and evaluated the climatic effect of solar system integration in three regions of Algeria: Algiers (coastal), Djelfa (highlands), and Tamanrasset (Sahara). The results showed a significant reduction in building loads (12%, 44%, and 22% for Algiers, Djelfa, and Tamanrasset, respectively) and a more than 60% solar energy

contribution for all cases. Additionally, it was noted that the solar percentage exceeds 45% when the optimal parameters of the solar system are chosen.

CHAPTER 3

SOLUTION METHODOLOGY

Developing solar combined cooling, heating, and power (SCCHP) systems is a viable approach to meet increasing energy needs and reducing environmental effects in pursuing sustainable energy solutions. This chapter examines the allowable domain of solar combined cooling, heating, and power (CCHP) systems, investigating the harmonious incorporation of solar technology with sophisticated energy conversion processes. Incorporating solar technology into combined cooling, heating, and power (SCCHP) systems can transform the energy sector, providing a flexible solution to various energy requirements. The growing need for energy security and environmental sustainability has sparked renewed interest in using solar energy's abundant and limitless potential. Traditional cooling, heating, and electricity production methods, which often depend on fossil fuels, substantially contribute to releasing greenhouse gases and the depletion of resources. In response to these difficulties, the notion of solar combination cooling, heating, and power (SCCHP) systems has arisen as a favorable alternative.

3.1. SYSTEM DESCRIPTION

In the present study, a SCCHP system is designed to meet the heating, cooling, and electricity demands of government institutions, large-scale hospitals, and residential complexes in Baghdad, Iraq. (Figure3. 1). During winter, a portion of the heating load is used for heating purposes, whereas during summer, a portion of the cooling load is utilized for cooling purposes. Hot water is essential year-round. The suggested system is a solar-powered organic Rankine cycle integrated cascaded vapor compression absorption refrigeration system. The suggested system has four subsystems: solar field and storage tank, ORC (Organic Rankine Cycle), Vapor

Absorption Refrigeration System (VARS), and Vapor Compression Refrigeration System (VCRS).

The solar field comprises parabolic trough collectors. The SPTC collector and thermal storage tank (TST) subsystem use therminol 66 as the heat transfer medium (HTF). A TST is used to provide uninterrupted energy provision throughout the whole day. The high-temperature heat transfer fluid (HTF) moves from the upper section of the thermal storage tank (TST) to the evaporator of the organic Rankine cycle (ORC) to provide thermal energy to the organic fluid.

In contrast, the cooled HTF leaves the TST's lower portion and flows into the SPTC's collector field. Once heated, the HTF is then circulated back to the upper part of the storage tank. The ORC subsystem employs n-octane as its working fluid. Exiting the ORT in a superheated state, the organic working fluid moves to the generator, where it releases heat, supplying energy for the subsequent vapor compression-absorption cycle. Additionally, the residual heat from the ORC's heat exchanger fulfills the heating requirements.

A cascade absorption-compression refrigeration system operates by utilizing two separate refrigerant circuits, each equipped with its own compressor and condenser. The absorption cycle acts within a circuit specifically constructed for lower temperatures, while the vapor compression cycle functions within a circuit optimized for higher temperatures.

During operation, the low-temperature circuit extracts heat from the chilled space using the evaporator and transmits it to the generator through a solution heat exchanger. The generator functions at elevated pressure and temperature, resulting in the vaporization and separation of the refrigerant from the solution.

The high-temperature circuit works similarly to a traditional vapor compression cycle, but its evaporator is connected to the condenser of the low-temperature circuit. The compressor in this circuit compresses the refrigerant gas, which then condenses

in the condenser and releases heat to the low-temperature circuit. The VCRS system use R410 as its working fluid, whereas the VARS system uses LiBr-H20.

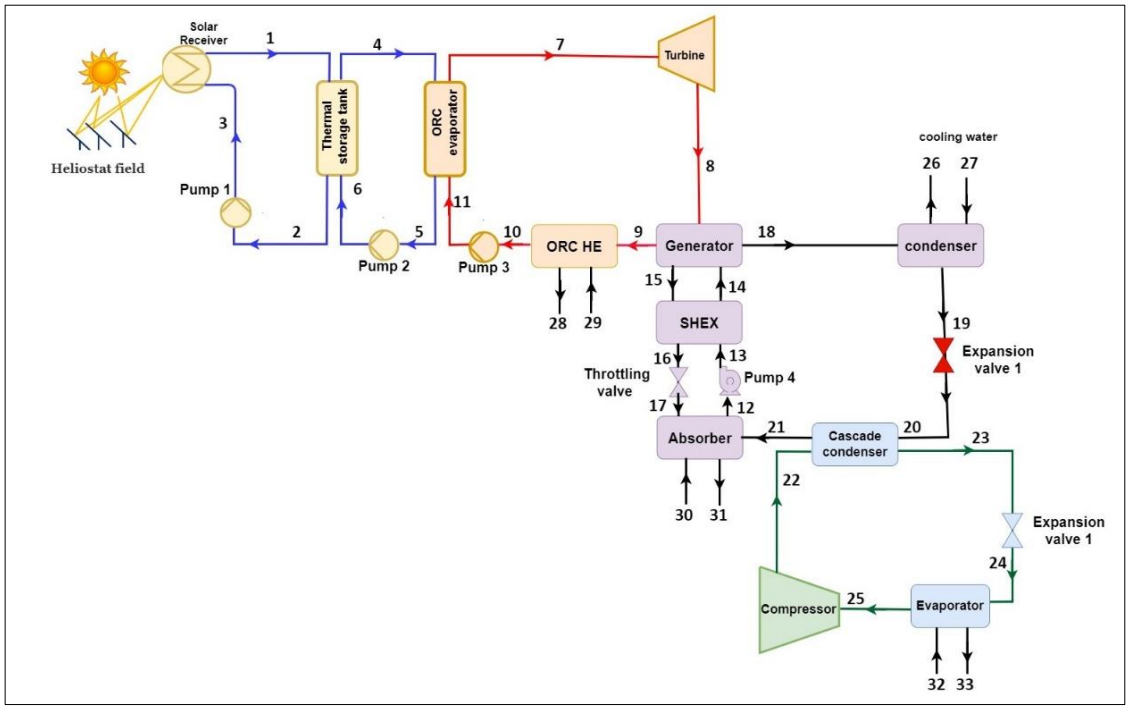

Figure 3.1. The schematic diagram for the SCCHP system.

3.2. THERMODYNAMIC MODELING OF THE RECOMMENDED SCCHP SYSTEM

The input data required for modeling the recommended SCCHP system are illustrated in Table 3.1. The modeling of the system is based on the following assumptions:

- All system components are supposed to operate in a condition of steady state.
- Kinetic, potential, and chemical exergies are disregarded.
- The fluids exiting the condenser and ORC heat exchanger are regarded as being in a saturated liquid state.
- The fluids exiting the evaporators are regarded as being in a saturated vapor state.
- All components' pressure drops, friction, and heat losses are ignored.

- Under certain temperature and pressure conditions, it is assumed that the LiBr-H_2O solutions in both the generator and the absorber are in a state of equilibrium.

Table 3.1. Input data for modeling of the suggested SCCHP.

Parameter	Value
Solar collectors area (m2)	510130 m2
Sun temperature	5770 K
Solar reservoir outlet temperature	243° C
Solar reservoir inlet temperature	127° C
Latitude (N)	33.18° N
Longitude (E)	44.21° E
Location	Baghdad-Iraq
Direct normal irradiation (DNI)	6.25 kWh/ m2.day
T_{amb}	25° C
P_{amb}	101kPa
Compressor inlet pressure (P25)	400 kPa
Compressor exit pressure (P22)	1200 kPa
Absorber temperature (T12)	36° C
Cascade condenser exit temperature (T21)	6.3° C
Generator temperature (T15)	90° C
LiBr solution strength	55%
Compressor efficiency	85%
ORC turbine efficiency	90%
ORC pump efficiency	80%

3.2.1. Energy and Exergy Analysis

For steady-flow open systems, mass, energy, and exergy balance relations can be listed as follows:

Mass (mass flow) balance per unit time [61,62]:

$$\sum \dot{m}_{in} = \sum \dot{m}_{out} \quad \text{(kg/s)} \tag{3.1}$$

where $\sum \dot{m}_{in}$ is the mass flow rate entering the system (kg/s), $\sum \dot{m}_{out}$ represents the mass flow rate (kg/s) coming out of the system.

Energy balance per unit time (energy flow balance)[63,64] :

$$\dot{E}_{in} - \dot{E}_{out} = \mathrm{dE}_{system}/dt \quad \text{(kW)} \tag{3.2}$$

where $\dot{E}_{in}$; the amount of energy entering the system per unit time (kW), $\dot{E}_{out}$; It refers to the amount of energy coming out of the system per unit time (kW), and dE_{system}/dt refers to the energy change per unit time. Exergy balance per unit time (exergy current balance) [65–67]:

$$\dot{EX}_{in} - \dot{EX}_{out} - \dot{EX}_{dis} = \mathrm{dEx}_{system}/dt \quad \text{(kW)} \tag{3.3}$$

And

$$\sum \left(1 - \frac{T_O}{T_K}\right) \dot{Q} - \dot{W} - \dot{EX}_W + \dot{EX}_{m,in} - \dot{EX}_{m,out} = \dot{EX}_{dis} \quad \text{(kW)} \tag{3.4}$$

And

$$\dot{EX}_Q - \dot{EX}_W + \sum \dot{m}_{in}\psi_{in} - \sum \dot{m}_{out}\psi_{out} = \dot{EX}_{dis} \quad \text{(kW)} \tag{3.5}$$

Equations 3.3-3.4 are three different equations expressing the exergy balance per unit time. In Equation 3.3. $\dot{EX}_{in}$; exergy entering the system per unit time; $\dot{EX}_{out}$: exergy leaving the system per unit time, $\dot{EX}_{dis}$; exergy destroyed in the system per unit time; dEx_{system}/dt; refers to the exergy change of the system over unit time.

Exergy current [68,69]:

$$\dot{EX} = \dot{m}\psi \quad \text{(kW)} \tag{3.6}$$

Equation 3.6 expresses the exergy flow occurring per unit time. $\dot{EX}$: exergy current (kW); $\dot{m}$: mass flow rate (kg/s); ψ: It refers to flow exergy or specific exergy (kJ/kg).

Specific exergy for each working fluid [70,71]:

$$\psi = (h - h_0) - T_0(s - s_0) \quad (3.7)$$

where h; enthalpy (kJ/kg), T; temperature (°C), s; The subscript “o” indicates entropy (kJ/kg K) and the dead state. The following section lists mass, energy, and exergy balance relations for SCCHP system components.

3.2.1.1. Thermal modeling of the ORC components

Organic Rankine Cycle Turbine Model

Figure 3.2 shows the ORT model, and the mass, energy, and exergy balance of the ORT model are listed as follows:

Figure 3.2. ORT model

Mass balance:

$$\dot{m}_7 = \dot{m}_8 \quad (3.8)$$

Energy balance:

$$\dot{W}_{ORT} = \dot{m}_8(h_7 - h_8) \quad (3.9)$$

Exergy balance:

$$\dot{EX}_{dis,ORT} = \dot{EX}_7 - \dot{EX}_7 - \dot{W}_{ORT} \quad (3.10)$$

Organic Rankine Heat Exchanger Model

The ORC heat exchanger model is shown in Figure 3.3. The following is a list of the mass, energy, and exergy balances for this model:

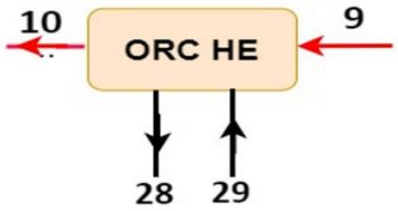

Figure 3.3. ORC HE model.

Mass balance:

$$\dot{m}_9 = \dot{m}_{10} \tag{3.11}$$

$$\dot{m}_{28} = \dot{m}_{29} \tag{3.12}$$

Energy balance:

$$\dot{Q}_{ORC\ HE} = \dot{m}_9(h_9 - h_{10}) = \dot{m}_{28}(h_{29} - h_{28}) \tag{3.13}$$

Exergy balance:

$$\dot{EX}_{dis,ORC\ HE} = \dot{EX}_9 - \dot{EX}_{10} + \dot{EX}_{28} - \dot{EX}_{29} \tag{3.14}$$

Organic Rankine Cycle Pump Model

Figure 3.4 presents the ORC pump model, and the mass, energy, and exergy balance of this model are listed as follows:

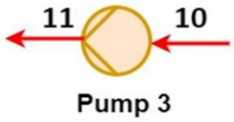

Figure 3.4. RC pump model

Mass balance:

$$\dot{m}_{10} = \dot{m}_{11} \tag{3.15}$$

Energy balance:

$$\dot{W}_{Pump\,3} = \dot{m}_{10}(h_{11} - h_{10}) \tag{3.16}$$

Exergy balance:

$$\dot{EX}_{dis,Pump\,3} = \dot{EX}_{10} - \dot{EX}_{11} + \dot{W}_{Pump\,3} \tag{3.17}$$

Organic Rankine Evaporator Model

The ORC evaporator model is shown in Figure 3.5. The following is a list of the mass, energy, and exergy balances for this model:

Figure 3.5. ORC evaporator model.

Mass balance:

$$\dot{m}_4 = \dot{m}_5 \tag{3.18}$$

$$\dot{m}_7 = \dot{m}_{11} \tag{3.19}$$

Energy balance:

$$\dot{Q}_{Evap\ 1} = \dot{m}_4(h_4 - h_5) = \dot{m}_7(h_7 - h_{11}) \quad (3.20)$$

Exergy balance:

$$\dot{EX}_{dis,Evap\ 1} = \dot{EX}_4 - \dot{EX}_5 + \dot{EX}_7 - \dot{EX}_{11} \quad (3.21)$$

3.2.1.2. Absorption Refrigeration Cycle (ARC) components

Generator Model

The generator model is presented in Figure 3.6. The following is a list of the mass, energy, and exergy balances for this model:

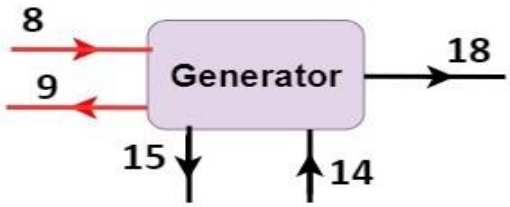

Figure 3.6. Generator model.

Mass balance:

$$\dot{m}_{14} = \dot{m}_{15} + \dot{m}_{18} \quad (3.22)$$

$$\dot{m}_8 = \dot{m}_9 \quad (3.23)$$

Energy balance:

$$\dot{Q}_{Gen} = \dot{m}_8(h_8 - h_9) = \dot{m}_{18}h_{18} + \dot{m}_{15}h_{15} - \dot{m}_{14}h_{14} \quad (3.24)$$

Exergy balance:

$$\dot{EX}_{dis,Gen} = \dot{EX}_8 - \dot{EX}_9 + \dot{EX}_{14} - \dot{EX}_{15} - \dot{EX}_{18} \quad (3.25)$$

Absorber Model

The absorber model is revealed in Figure 3.7. The following is a list of the mass, energy, and exergy balances for this model:

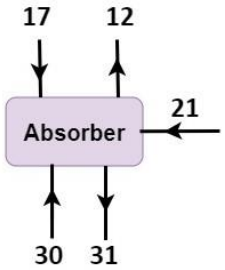

Figure 3.7. Absorber model.

Mass balance:

$$\dot{m}_{17} + \dot{m}_{21} = \dot{m}_{12} \quad (3.26)$$

$$\dot{m}_{30} = \dot{m}_{31} \quad (3.27)$$

Energy balance:

$$\dot{Q}_{Abs} = \dot{m}_{31}(h_{31} - h_{30}) = \dot{m}_{17}h_{17} + \dot{m}_{21}h_{21} - \dot{m}_{12}h_{12} \quad (3.28)$$

Exergy balance:

$$\dot{EX}_{dis,Abs} = \dot{EX}_{21} + \dot{EX}_{17} - \dot{EX}_{12} + \dot{EX}_{30} - \dot{EX}_{31} \quad (3.29)$$

Absorption Refrigeration Cycle Pump Model (Pump 4)

Figure 3.8 presents the ARC pump model, and the mass, energy, and exergy balance of this model are listed as follows:

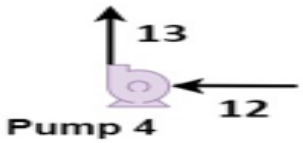

Figure 3.8. ARC pump model

Mass balance:

$$\dot{m}_{12} = \dot{m}_{13} \tag{3.30}$$

Energy balance:

$$\dot{W}_{Pump\ 4} = \dot{m}_{12}(h_{13} - h_{12}) \tag{3.31}$$

Exergy balance:

$$\dot{EX}_{dis,Pump\ 4} = \dot{EX}_{12} - \dot{EX}_{13} + \dot{W}_{Pump\ 4} \tag{3.32}$$

Throttling Valve Model

Figure 3.9 illustrates the ARC throttling valve model, and the mass, energy, and exergy balance of this model are summarized as follows:

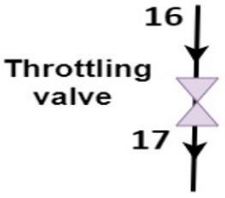

Figure 3.9. ARC Throttling valve model

Mass balance:

$$\dot{m}_{16} = \dot{m}_{17} \tag{3.33}$$

Energy balance:

$$h_{16} = h_{17} \tag{3.34}$$

Exergy balance:

$$\dot{EX}_{dis,PRV} = \dot{EX}_{16} - \dot{EX}_{17} \tag{3.35}$$

Sensible Heat Exchanger Model

The sensible heat exchanger model is shown in Figure 3.10. The following is a summary of the mass, energy, and exergy balances for this model:

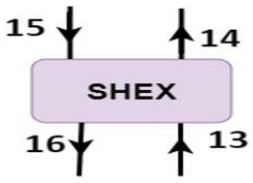

Figure 3.10. Sensible heat exchanger (SHEX) model

Mass balance:

$$\dot{m}_{13} = \dot{m}_{14} \tag{3.36}$$

$$\dot{m}_{15} = \dot{m}_{16} \tag{3.37}$$

Energy balance:

$$\dot{Q}_{SHEX} = \dot{m}_{13}(h_{14} - h_{13}) = \dot{m}_{15}(h_{15} - h_{16}) \tag{3.38}$$

Exergy balance:

$$\dot{EX}_{dis,SHEX} = \dot{EX}_{13} - \dot{EX}_{14} + \dot{EX}_{15} - \dot{EX}_{16} \quad (3.39)$$

Cascade Condenser Model

The ARC cascade condenser model is presented in Figure 3.11. The following is a list of the mass, energy, and exergy balances for this model:

Figure 3.11. Cascade condenser model.

Mass balance:

$$\dot{m}_{20} = \dot{m}_{21} \quad (3.40)$$

$$\dot{m}_{22} = \dot{m}_{23} \quad (3.41)$$

Energy balance:

$$\dot{Q}_{Cascade} = \dot{m}_{21}(h_{21} - h_{20}) = \dot{m}_{23}(h_{22} - h_{23}) \quad (3.42)$$

Exergy balance:

$$\dot{EX}_{dis,Cascade} = \dot{EX}_{20} - \dot{EX}_{21} + \dot{EX}_{22} - \dot{EX}_{23} \quad (3.43)$$

Condenser Model

The ARC condenser model is illustrated in Figure 3.12. The following is a list of the mass, energy, and exergy balances for this model:

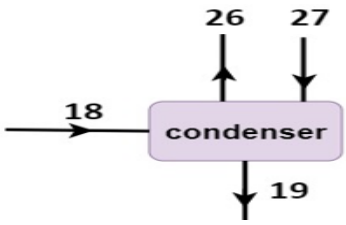

Figure 3.12. ARC condenser model.

Mass balance:

$$\dot{m}_{18} = \dot{m}_{19} \tag{3.44}$$

$$\dot{m}_{26} = \dot{m}_{27} \tag{3.45}$$

Energy balance:

$$\dot{Q}_{Cond} = \dot{m}_{18}(h_{18} - h_{19}) = \dot{m}_{26}(h_{27} - h_{26}) \tag{3.46}$$

Exergy balance:

$$\dot{EX}_{dis,Cond} = \dot{EX}_{18} - \dot{EX}_{19} + \dot{EX}_{26} - \dot{EX}_{27} \tag{3.47}$$

Expansion Valve 1 (EV1) Model

Figure 3.13 illustrates EV1 model for the ARC system, and the mass, energy, and exergy balance of this model are listed as follows:

Figure 3.13. Expansion valve model for ARC

Mass balance:

$$\dot{m}_{19} = \dot{m}_{20} \tag{3.48}$$

Energy balance:

$$h_{19} = h_{20} \tag{3.49}$$

Exergy balance:

$$\dot{EX}_{dis,EV1} = \dot{EX}_{19} - \dot{EX}_{20} \tag{3.50}$$

3.2.1.3. Vapor Compression Refrigeration Cycle (VCRC) Components

Evaporator Model

The evaporator model for the VCRC system is shown in Figure 3.14. The following is a list of the mass, energy, and exergy balances for this model:

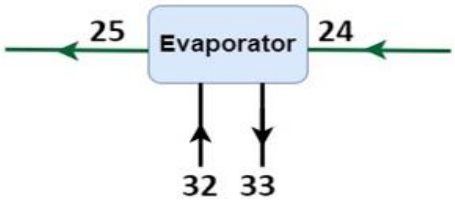

Figure 3.14. Evaporator model for VCRC cycle.

Mass balance:

$$\dot{m}_{24} = \dot{m}_{25} \tag{3.51}$$

$$\dot{m}_{32} = \dot{m}_{33} \tag{3.52}$$

Energy balance:

$$\dot{Q}_{Evap\,2} = \dot{m}_{24}(h_{25} - h_{24}) = \dot{m}_{33}(h_{32} - h_{33}) \quad (3.53)$$

Exergy balance:

$$\dot{EX}_{dis,Evap\,2} = \dot{EX}_{24} - \dot{EX}_{25} + \dot{EX}_{32} - \dot{EX}_{33} \quad (3.54)$$

Expansion Valve (EV2) Model

Figure 3.15 presents EV2 model for the VCRC system, and the mass, energy, and exergy balance of this model are listed as follows:

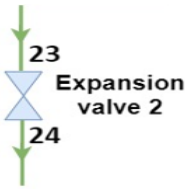

Figure 3. 15. Expansion valve model for VCC

Mass balance:

$$\dot{m}_{23} = \dot{m}_{24} \quad (3.55)$$

Energy balance:

$$h_{23} = h_{24} \quad (3.56)$$

Exergy balance:

$$\dot{EX}_{dis,EV2} = \dot{EX}_{23} - \dot{EX}_{24} \quad (3.57)$$

Compressor Model

Figure 3.16 presents the compressor model, and the mass, energy, and exergy balance of this model are listed as follows:

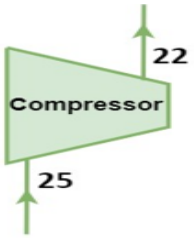

Figure 3. 16. Compressor model

Mass balance:

$$\dot{m}_{25} = \dot{m}_{22} \tag{3.58}$$

Energy balance:

$$\dot{W}_{Comp} = \dot{m}_{22}(h_{22} - h_{25}) \tag{3.59}$$

Exergy balance:

$$\dot{EX}_{dis,Com} = \dot{EX}_{25} - \dot{EX}_{22} + \dot{W}_{Com} \tag{5.60}$$

3.2.1.4. Solar Filed and Tank Modelling

Solar Power Tower (SPTC)

SPTC technology has risen to prominence among all CSP systems because of its capacity to produce higher concentration rates and create thermal energy at higher temperatures than PTC technology, as well as its faster adoption of thermal storage than PV technology. This has prompted the use of SPT technology to store thermal energy at high temperatures for polygeneration applications. Figure 3.17 presents the SPTC model, and the mass, energy, and exergy balance of this model are listed as follows:

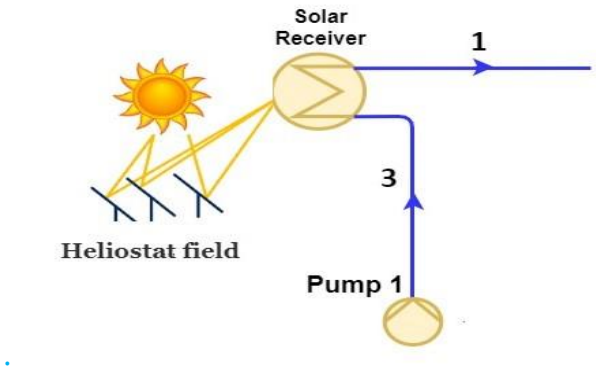

Figure 3.17. Solar power tower (SPTC) model.

Mass balance:

$$\dot{m}_3 = \dot{m}_1 \tag{3.61}$$

Energy balance

$$\dot{Q}_{\text{Solar}} = A_h . DNI . N_h \tag{3.62}$$

$$\dot{Q}_{\text{Solar, in}} = \dot{Q}_{\text{Solar}} . \eta_h = \dot{m}_1 (h_1 - h_3) \tag{3.63}$$

Exergy balance

$$\dot{E}_{D,SR} = \left(\dot{EX}_3 - \dot{EX}_1\right) + \dot{E}_{Q,Solar} \tag{3.64}$$

$$\dot{E}_{Q,Solar} = \dot{Q}_{solar} \left(1 - \frac{T_0}{T_{sun}}\right) \tag{3.65}$$

Thermal Energy Storage (TST)

Thermal energy storage is the process of raising or lowering the temperature of a substance in order to store energy for future use. This technology has the capability to equilibrate energy usage between the daytime and overnight periods. Figure 3.18

presents the TST model, and the mass, energy, and exergy balance of this model are listed as follows:

Figure 3.18. Thermal energy storage (TST) model.

Mass balance:

$$\dot{m}_1 = \dot{m}_2 \tag{3.66}$$

$$\dot{m}_6 = \dot{m}_4 \tag{3.67}$$

Energy balance [72]**:**

$$\dot{Q}_{\mathrm{St}} = \dot{Q}_{\mathrm{TST,in}} - \dot{Q}_{\mathrm{Loss}} - \dot{Q}_{Evap\ 1} \tag{3.68}$$

$$\dot{Q}_{\mathrm{St}} == \rho.\mathrm{V}.\ C_p.\frac{dT_{st}}{dt} \tag{3.69}$$

$$\dot{Q}_{\mathrm{TST,in}} = \dot{m}_1(h_1 - h_2) \tag{3.70}$$

$$\dot{Q}_{\mathrm{loss}} == \mathrm{A}_t.\mathrm{u}_t.\ (T_{st} - T_{amb}) \tag{3.71}$$

Exergy balance

$$\dot{E}_{D,St} = \dot{EX}_1 - \dot{EX}_2 + \dot{EX}_6 - \dot{EX}_4 \tag{3.72}$$

Pump1 Model

Figure 3.19 presents the ARC pump model, and the mass, energy, and exergy balance of this model are listed as follows:

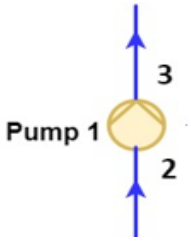

Figure 3.19. Pump1 model

Mass balance:

$$\dot{m}_2 = \dot{m}_3 \tag{3-73}$$

Energy balance:

$$\dot{W}_{Pump\,1} = \dot{m}_2(h_3 - h_2) \tag{3.74}$$

Exergy balance:

$$\dot{EX}_{dis,Pump\,1} = \dot{EX}_2 - \dot{EX}_3 + \dot{W}_{Pump\,1} \tag{3.75}$$

Pump2 Model

Figure 3.20 presents the pump2 model, and the mass, energy, and exergy balance of this model are listed as follows:

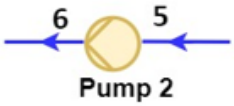

Figure 3.20. Pump2 model

Mass balance:

$$\dot{m}_5 = \dot{m}_6 \tag{3.76}$$

Energy balance:

$$\dot{W}_{Pump\,2} = \dot{m}_5(h_6 - h_5) \tag{3.77}$$

Exergy balance:

$$\dot{EX}_{dis,Pump\,2} = \dot{EX}_5 - \dot{EX}_6 + \dot{W}_{Pump\,2} \tag{3.78}$$

3.2.2. Thermal Performance

The system's total thermal efficiency is given by[73]:

$$\eta_{\mathrm{SCCHP}} = \frac{\dot{W}_{net}+\dot{Q}_{heating}+\dot{Q}_{cooling}}{A_h.DNI.N_h} \tag{3.79}$$

Here is the system's Wok net:

$$\dot{W}_{net} = \dot{W}_{ORT} - \dot{W}_{compressor} - \dot{W}_{Pump\,1} - \dot{W}_{Pump\,2} - \dot{W}_{Pump\,3} - \dot{W}_{Pump\,4} \tag{3.80}$$

The system's total exergy efficiency is given by[74]:

$$\psi_{\mathrm{SCCHP}} = \frac{\dot{W}_{net}+\dot{EX}_{P,heating}+\dot{EX}_{P,cooling}}{\dot{EX}_{Sun}} \tag{3.81}$$

The coefficient of performance of the refrigeration cycles is given by the following equations:

$$\mathrm{COP}_{\mathrm{VCRS}} = \frac{\dot{Q}_{Evaporator}}{\dot{W}_{compressor}} \tag{3.82}$$

$$\mathrm{COP}_{\mathrm{VARS}} = \frac{\dot{Q}_{cascade\ condenser}}{\dot{Q}_{Generator}+\dot{W}_{Pump\,4}} \tag{3.83}$$

$$\mathrm{COP}_{\mathrm{VCARS}} = \frac{\dot{Q}_{Evaporator}}{\dot{Q}_{Generator}+\dot{W}_{Pump\ 4}+\dot{W}_{compressor}} \quad (3.84)$$

3.3. EXERGO-ECONOMIC MODELING of the RECOMMENDED SCCHP SYSTEM

The following is the general balance equation for component cost analysis [75–77]:

$$\sum \dot{C}_{in,k} + \dot{C}_{Qk} + \dot{Z}_k = \sum \dot{C}_{out,k} + \dot{C}_{w,k} \quad (3.85)$$

Exergy cost (Equation 3.86-3.90) [78];

$$\dot{C} = c\dot{E}x \quad (3.86)$$

$$\dot{C}_{D,k} = c_f \dot{E}x_{D,k} \quad (3.87)$$

$$\dot{C} = c\dot{E}x \quad (3.88)$$

$$\dot{C}_Q = c\dot{E}_Q \quad (3.89)$$

$$\dot{C}_W = c\dot{W} \quad (3.90)$$

The capital investment cost is calculated according to the following equations [79–82]:

$$\dot{Z}_k = Z_k^{CI} * CRF * \frac{\phi}{t} \quad (3.91)$$

$$CRF = \frac{i(1+i)^N}{(1-i)^N - 1} \quad (3.92)$$

All the cost and capital investment cost equations for the SCCHP system are given in Table 3.2.

Here, the equation that determines the exergy-economic factor (f_k):

$$f_k = \frac{\dot{Z}_k}{\dot{Z}_k + \dot{C}_{D,k}} \tag{3.93}$$

The total cost of the system ($\dot{C}_{system}$) may be calculated using the equation provided [83,84]:

$$\dot{C}_{system} = \sum \dot{z}_k + \sum \dot{C}_{D,k} \tag{3.94}$$

Table 3.2. Cost balance equations for the SCCHP system components.

Components	Cost equation	Auxiliary Equations	Investment Cost
SPTC	$\dot{C}_3 + \dot{Z}_{SPTC} = \dot{C}_1$		$\dot{Z}_{SPTC} = 126.\,A_h$
TES	$\dot{C}_1 + \dot{C}_6 + \dot{Z}_{TST} = \dot{C}_2 + \dot{C}_4 + \dot{C}_{TST}$	$c_1 = c_2$	$\dot{Z}_{PTC} = 1380.\,V_{TST}^{0.4^{0.4}}$ $V_{TST} = = 126.\,A_h/30$
Pump 1	$\dot{C}_2 + \dot{Z}_{P1} = \dot{C}_3$		$\dot{Z}_{P1} = 3450\,\dot{W}_{pump1}^{0.71}$
Pump 2	$\dot{C}_5 + \dot{Z}_{P2} = \dot{C}_6$		$\dot{Z}_{Pump2} = 3450\,\dot{W}_{pump2}^{0.71}$
ORT	$\dot{C}_7 + \dot{Z}_{ORT} = \dot{C}_8 + \dot{C}_{ORT}$	$c_7 = c_8$ $c_{ORT} = c_{P1}$	$\dot{Z}_{ORT} = (479.34 \times \dot{m}_7/0.92 - \eta_T)\mathrm{Ln}(p_7/p_8)\,(1 + \exp(0.036 \times T_7 - 54.4))$
ORC HE	$\dot{C}_9 + \dot{C}_{28} + \dot{Z}_{ORC\,HE} = \dot{C}_{10} + \dot{C}_{29} + \dot{C}_{ORC\,HE}$	$\frac{\dot{C}_9}{\dot{E}X_9} = \frac{\dot{C}_{10}}{\dot{E}X_{10}}$ $c_{28} = 0$	$\dot{Z}_{ORC\,HE} = 235.\,\dot{Q}_{ORC\,HE}$
Pump 3	$\dot{C}_{10} + \dot{Z}_{P3} = \dot{C}_{11}$		$\dot{Z}_{P3} = 3450\,\dot{W}_{pump3}^{0.71}$
Generator	$\dot{C}_{14} + \dot{C}_8 + \dot{Z}_{Gen} = \dot{C}_{15} + \dot{C}_9 + \dot{C}_{18}$	$\frac{\dot{C}_8 - \dot{C}_{14}}{\dot{E}X_8 - \dot{E}X_{14}} = \frac{\dot{C}_{15} - \dot{C}_{14}}{\dot{E}X_{15} - \dot{E}X_{14}}$	$\dot{Z}_{Gen} = 190 + 130\,A_{Gen}$
SHEX	$\dot{C}_{13} + \dot{C}_{15} + \dot{Z}_{SHEX} = \dot{C}_{14} + \dot{C}_{16}$	$c_{13} = c_{14}$	$\dot{Z}_{SHEX} = 190 + 130\,A_{SHEX}^{0.85}$
Absorber	$\dot{C}_{17} + \dot{C}_{30} + \dot{C}_{21} + \dot{Z}_{Abs} = \dot{C}_{12} + \dot{C}_{31}$	$\frac{\dot{C}_{12}}{\dot{E}X_{12}} = \frac{\dot{C}_{17} - \dot{C}_{21}}{\dot{E}X_{17} - \dot{E}X_{21}}$ $c_{30} = 0$	$\dot{Z}_{Abs} = 190 + 130\,A_{Abs}$
Pump 4	$\dot{C}_{12} + \dot{Z}_{P4} = \dot{C}_{13}$		$\dot{Z}_{Pump4} = 3450\,\dot{W}_{pump4}^{0.71}$
PRV	$\dot{C}_{16} + \dot{Z}_{PRV} = \dot{C}_{17}$		$\dot{Z}_{PRC} = 114.5.\,\dot{m}_{16}$
Condenser	$\dot{C}_{18} + \dot{C}_{26} + \dot{Z}_{cond} = \dot{C}_{19} + \dot{C}_{27}$	$c_{18} = c_{18}$	$\dot{Z}_{cond} = 1173.\,\dot{m}_{18}$
Cascade cond.	$\dot{C}_{20} + \dot{C}_{22} + \dot{Z}_{cascade} = \dot{C}_{21} + \dot{C}_{23}$	$c_{22} = c_{23}$	$\dot{Z}_{cascade} = 16000.\left(A_{Cascade}/_{1000}\right)^{0.6}$
Compressor	$\dot{C}_{25} + \dot{C}_C + \dot{Z}_C = \dot{C}_{22}$	$c_{ORT} = c_c$	$\dot{Z}_C = (71.1 \times \dot{m}_{22}/0.9 - \eta_c)(p_{22}/p_{25})\mathrm{Ln}(p_{22}$

EV1	$\dot{C}_{19} + \dot{Z}_{EV1} = \dot{C}_{20}$	$\dot{Z}_{EV1} = 114.5.\ \dot{m}_{19}$
EV2	$\dot{C}_{16} + \dot{Z}_{PRV} = \dot{C}_{17}$	$\dot{Z}_{EV2} = 114.5.\ \dot{m}_{23}$
Evaporator	$\dot{C}_{24} + \dot{C}_{32} + \dot{Z}_{Evap2} = \dot{C}_{25} + \dot{C}_{33}$ $c_{24} = c_{25}$	$\dot{Z}_{Evap2} = 16000.\left(A_{Evap2}/1000\right)^{0.6}$
ORC Evaporator	$\dot{C}_4 + \dot{C}_{11} + \dot{Z}_{Evap1} = \dot{C}_7$ $c_4 = c_5$ $+ \dot{C}_5$	$\dot{Z}_{Evap1} = 16000.\left(A_{Evap1}/1000\right)^{0.6}$

CHAPTER 4

RESULTS AND DISCUSSION

This chapter delves into the discussion of energy, exergy, and exergo-economic analysis within the SCCHP components. The preceding chapters laid the groundwork, introducing the system, its operation, and the theoretical underpinnings of the applied thermodynamics fundamentals and laws for each component of the SCCHP system.

The results begin with energy analysis, tracing the energy flows through the system, exergy losses, and exergo-economic for each component, and pinpointing areas for potential improvement. The efficiency of each component is presented, revealing where valuable energy dissipates as exergy destruction. This lays the foundation for understanding the actual quality of energy available. Table 4.1 displays each state point's calculated and presumed characteristics in the SCCHP system. Also, Table 4.2 provides the calculated values for Enthalpy, entropy, exergy, and cost of the SCCHP states.

Table 4.1. The properties for each state for the SCCHP states.

State	m (kg/s)	Fluid	Pressure (kPa)	Temperature (K)	X (%)
1	19.42	Therminol_66	7	243	
2	19.42	Therminol_66	7	127	
3	19.42	Therminol_66	1.5	127.1	
4	19.42	Therminol_66	6	233	
5	19.42	Therminol_66	2	120.1	
6	19.42	Therminol_66	6	120.2	
7	12.18	n-octane	85	120	
8	12.18	n-octane	35	107.9	
9	12.18	n-octane	35	91.22	
10	12.18	n-octane	35	91.22	
11	12.18	n-octane	85	91.24	
12	0.7506	LiBr-water	0.9577	36	0.55
13	0.7506	LiBr-water	6	36.02	0.55
14	0.7506	LiBr-water	6	49.03	0.55
15	0.6255	LiBr-water	6	90.22	0.66
16	0.6255	LiBr-water	6	79.38	0.66
17	0.6255	LiBr-water	0.9577	58.34	0.66
18	0.1251	Water	6	90.22	
19	0.1251	Water	6	36.16	
20	0.1251	Water	0.9577	6.342	
21	0.1251	Water	0.9577	6.342	
22	1.289	R410a	1200	35.33	
23	1.289	R410a	1200	13.35	
24	1.289	R410a	400	-20.03	
25	1.289	R410a	400	-19.95	
26	15.07	Water	101	25	
27	15.07	Water	101	30	
28	94.31	Water	101	70	
29	94.31	Water	101	80	
30	18.79	Water	101	25	

31	18.79	Water	101	30
32	31.08	Air	101	-8
33	31.08	Air	101	-16

Table 4. 2. Enthalpy, entropy, exergy, and cost for the SCCHP states.

State	Enthalpy (kJ/kg)	Entropy (kJ/kg.K)	Exergy (MW)	Cost ($/hr)
1	476	1.229	2245	57.45
2	227.7	0.6864	530.3	13.57
3	227.9	0.6869	531.2	13.91
4	452.7	1.183	2052	57.47
5	214.5	0.653	465.6	13.04
6	214.7	0.6535	466.6	13.39
7	535.7	1.446	1277	52.6
8	514	1.452	990	40.77
9	480.8	1.363	908.9	37.43
10	155.9	0.4717	187.1	7.703
11	156	0.4718	188.1	7.831
12	86.31	0.2195	36.41	3.66
13	86.34	0.2196	36.41	3.666
14	112.8	0.3036	37.47	3.772
15	248	0.4691	84.96	3.595
16	228.9	0.4157	82.99	3.497
17	228.9	0.4158	82.98	3.498
18	2669	8.635	12.58	3.865
19	151.5	0.5208	0.09751	0.02995
20	151.5	0.5431	-0.732	0.03017
21	2513	8.991	-20.29	2.803
22	449.8	1.869	102.5	2.622
23	220.7	1.073	-0.07535	0.001927
24	220.7	1.088	-5.727	0.0003707
25	414.2	1.852	63.28	0.004097

26	104.9	0.3672	0	0
27	125.8	0.4367	2.769	3.838
28	293.1	0.9551	1221	0
29	335	1.076	1792	34.89
30	104.9	0.3672	0	0
31	125.8	0.4367	3.453	2.762
32	265.5	5.579	61.01	0
33	257.4	5.548	96.22	0.09258

4.1. MODEL VERIFICATION

Two parts of the whole system were compared with the references to assess the correctness of the suggested modeling. Table 4.3 compares the findings of the ORC-powered cascaded vapor compression absorption refrigeration system to the numerical results derived from Ref. [85]. Table 4.4 compares the findings of the solar ORC modeling to the experimental data derived from Ref. [86]. The findings of this investigation are in good accord with the findings of the cited literature.

Table 4.3. Validation outcomes for the ORC-driven cascaded vapor compression absorption refrigeration system.

	Model of Ref. [85]	**Present model**	**Deviation (%)**
$\dot{W}_{\text{compressor}}$ **(kW)**	8.15	8.31	1.92
$\dot{Q}_{\text{cascade condenser}}$ **(kW)**	3.76	3.72	1.07
$\dot{Q}_{\text{evaporator1}}$ **(kW)**	30.6	30.8	0.65
$\dot{Q}_{\text{absorber}}$ **(kW)**	47.75	49.53	3.6
$\dot{Q}_{\text{generator}}$ **(kW)**	49.95	50.87	1.81
$\dot{Q}_{\text{ORC HX}}$ **(kW)**	77.99	75.49	3.3
$\dot{Q}_{\text{SHEX}}$ **(kW)**	11.21	11.44	2.01
$\dot{Q}_{\text{condenser}}$ **(kW)**	39.86	39.79	0.176
$\dot{W}_{\text{pump4}}$ **(kW)**	0.58	0.591	1.86
$\dot{W}_{\text{turbine}}$ **(kW)**	10.20	10.23	0.293

$\dot{Q}_{\text{ORC evaporator}}$ (kW)	137.60	135.17	0.411
η_I	80.05	79.62	0.54
COP_{VARS}	0.75	0.76	1.32
COP_{VCRS}	3.76	4.46	1.57

Table 4.4. ORC subsystem validation findings.

	Model of Ref [86]	Present model	Absolute Deviation (%)
$\dot{W}_{ORT}$ (kW)	2.03	2.028	0.1
$\dot{Q}_{condenser}$ (kW)	26.51	26.57	0.226
$\dot{Q}_{\text{ORC evaporator}}$ (kW)	33.54	32.93	1.85
$\eta_{\text{I,ORC}}$ (%)	6.04	5.97	1.7
$\eta_{\text{I,CCHP}}$ (%)	72.26	72.13	0.18

4.2. RESULTS OF ENERGY AND EXERGOECONOMIC AT DESIGN CONDITIONS

Under ideal operating conditions, the exergy analysis results for the SCCHP components are displayed in Figure 4.1 and Table 4.5. Essential information regarding the sources of irreversibility is provided in Table 4.5. The solar collector produces the highest exergy destruction rate, 3769 kW, as shown in Table 3. The total cooling load provided by the evaporator is 249.4 kW, while the total heating load provided by the ORC heat exchanger is 3956 kW, as shown in Table 4.5. The power produced by the ORC turbine is 264.3 kW, while the compressor and pumps consume 20.7% of this power. The compressor consumed 45.94 kW, whereas the pumps consumed 8.883 kW.

Table 4. 5. Energy and exergy analysis for each component of the model for octane

Component	$\dot{E}_D$ (kW)	$\dot{E}_D$ (%)	Ψ (%)	$\dot{Q}$ or $\dot{W}$ (kW)
SPTC	3769	77.42	31.25	4817
TST	128.7	2.643	92.5	4800
Pump1	2.76	0.0566	24.81	3.88
ORC evaporator	497.3	10.21	68.7	4624
Pump2	2.77	0.0569	26.89	3.79
ORC turbine	23	0.472	92	264.3
ORC HE	150.9	3.1	79.1	3956
Pump3	0.194	0.004	83.64	1.185
Generator	21.01	0.431	74/1	404.4
Condenser	9.717	0.2	22.18	315
EV1	0.83	0.017	88.25	0
Cascade cond.	122.1	2.51	19.07	295.4
Absorber	22.82	0.469	13.14	392.8
Pump 4	0.0272	0.0006	3.314	0.028
EV2	5.652	0.116	98.3	0
SHEX	0.91	0.0187	53.8	11.91
PRV	0.019	0.0004	99.9	0
Evaporator	104.2	2.141	51.03	249.4
Compressor	6.711	0.138	85.4	45.94

Figure 4.1 presents the total exergy destruction as a function of all components (excluding the collector). The highest exergy destruction occurs by solar collectors. It is shown from this figure that the highest exergy destruction, except for collectors, appears by the ORC evaporator and the ORC heat exchanger due to high heat transfer rates. They make up 45.3% and 13.8 %, respectively.

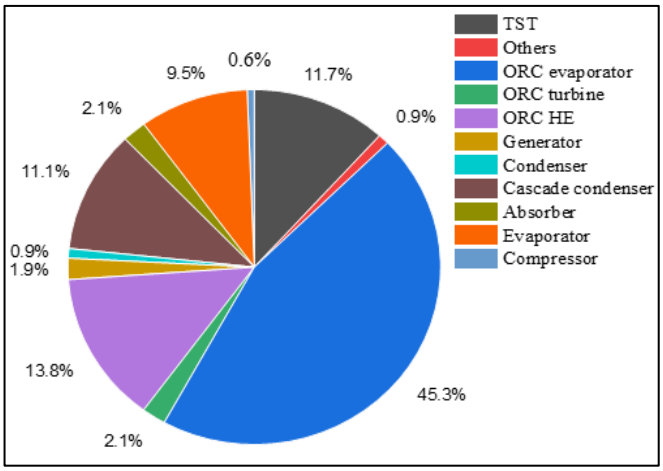

Figure 4.1. Total exergy destruction as a function of all components (excluding collector).

The exergo-economic parameters for the SCCHP system can be found in Table 4.6. The exergo-economic analysis shows that the total investment cost of the CCHP system is 83.67 $/h, and the cost of total exergy destruction is 31.7 $/h. An exergo-economic factor (f) of 63.315% is computed for the entire system. The SPTC has the highest capital cost rate ($\dot{Z}_k + \dot{C}_{D,k}$) among all the components due to its large area, amounting to 43.53 $/h. The second highest capital cost rates are the ORC evaporator and ORC heat exchanger, which are 14.26 $/h and 8.037 $/h, respectively. The ORC turbine and TST exhibit comparatively high capital cost rates, with rates of 3.634 $/h and 3.5 $/h, respectively. The ARC condenser and cascade condenser also play a role in the plant's capital expenses, with rates of 2.99 $/h and 2.4 $/h. The capital cost rates for the remaining components of the system are minimal.

Table 4.6 presents the exergy destruction cost rate ($\dot{C}_{D,k}$), an essential factor in exergoeconomic analysis. It is demonstrable that the ORC evaporator possesses the highest $\dot{C}_D$ at 13.93 $/h. Next to the ORC evaporator, the ORC heat exchanger is the most important component, and it has a relatively high $\dot{C}_D$ value.

Table 4.6. Exergo-economic results of components of (CCHP) system.

Component	$\dot{C}_{D,k}$(\$/h)	$\dot{Z}_k$ (\$/h)	$\dot{Z}_k + \dot{C}_{D,k}$ (\$/h)	f (%)
SPTC	0	43.53	43.53	100
TST	1.55	1.954	3.5	55.83
Pump1	0.1513	0.139	0.29	47.8
ORC evaporator	13.93	1.426	14.26	2.37
Pump2	0.1522	0.142	0.294	48.3
ORC turbine	0.947	2.69	3.634	73.94
ORC HE	6.213	1.824	8.037	22.7
Pump3	0.0106	0.0623	0.073	85.4
Generator	0.865	0.35	1.214	28.75
ARC Condenser	2.896	0.0945	2.99	3.16
EV1	0.255	0.00022	0.255	0.087
Cascade cond.	1.766	0.6275	2.393	26.221
Absorber	2.292	0.0121	2.413	5.017
Pump 4	0.0015	0.00244	0.006	74.5
EV2	0.1445	0.0023	0.147	1.565
SHEX	0.0454	0.0086	0.054	15.46
PRV	0.0018	0.00011	0.0019	5.866
Evaporator	0.085	0.0154	0.1	15.4
Compressor	0.3824	0.094	0.476	19.74
Total	31.689	52.97	83.67	63.315

4.3. PARAMETRIC STUDY

4.3.1 Effect of ORC working fluid

To assess the impact of changing the ORC working fluid, all system operating conditions are kept constant except for the working fluid itself and the resulting pressure ratio (Pr) variations in the ORC. The pressure ratio employed in this investigation is analogous to the Pr utilized in another research on ORC. The organic working fluid is in a superheated state at the exit of the turbine for the selected

working fluids. The evaporation and condensation pressures of the ORC for various working fluids utilized in this investigation are shown in Table 4.7.

Table 4.7. ORC condensation and evaporation pressures for various operating fluids

Working Fluid	Evaporation pressures (kPa)	Condensation pressures (kPa)
Pentane	810	490
Butane	2000	1200
R245fa	1800	1000
NDM	38	13
Octane	80	35

According to Table 4.8, the energy and exergy efficiencies of the SCCHP system are almost identical, while the system with R245fa is more efficient in terms of energy. The R245fa system has the lowest exergy destruction rate and the best thermal and exergy efficiency. Octane and butane have the lowest investment cost and the lowest cost of exergy destruction, respectively. In all cases, the factor f is greater than 55%, with octane having the greatest value (63.32).

Table 4.8. Energy, exergy, and exergo-economic results of the CCHP system for the examined organic fluids.

Working Fluid	η_I (%)	ψ (%)	$\dot{E}_{D,T}$ (kW)	$\dot{Z}_{D,T}$ ($/hr)	$\dot{C}_{D,T}$ ($/hr)	$\dot{Z}_{D,T} + \dot{C}_{D,T}$ ($/hr)	f (%)
Pentane	76.33	17.14	4801	48.96	35.57	84.53	57.92
Butane	76.56	16.94	4773	49.48	34.33	83.81	59.04
R245fa	77.24	17.53	4737	51.63	33.3	84.93	60.79
NDM	73.55	16.2	4897	52.8	42.62	95.43	55.33
Octane	76.37	17.75	4759	52.97	31.7	83.67	63.32

Table 4.9 presents the SCCHP system output results for various organic fluids. These results include the work net output, heating, and cooling loads. The results showed that the maximum work net and heating load are provided by octane and R245fa, while the MDM offers the highest value of the cooling load.

Table 4.9. The SCCHP system output results for various organic fluids.

Working Fluid	$\dot{W}_{net}$ (kW)	$\dot{Q}_{heating}$ (kW)	$\dot{Q}_{cooling}$ (kW)	COP_{VCRS}	COP_{VARS}	COP_{VACRS}
Pentane	161.9	3999	251.5	5.43	0.729	0.553
Butane	187.9	3999	239.4	5.43	0.736	0.558
R245fa	201.1	4076	188.4	5.43	0.7331	0.556
NDM	167.8	3627	457.4	5.43	0.735	0.557
Octane	209.7	3965	249.4	5.43	0.73	0.554

Also, Table 4.10 reveals the total cost for each individual system in the CCHP system for various organic fluids. The findings clearly show that more than 50 % of the total cost rate is needed for the SPTC system. The SCCHP system with MDM has the highest total cost rate ($\dot{C}_T$) among all the working fluids (about 43.53 $/h), whereas the real cost rate of the CCHP system with other working fluids is almost equal.

Table 4.10. The total cost for each individual system in the CCHP system for various organic fluids.

Working Fluid	$\dot{C}_{SPTC}$ ($/hr)	$\dot{C}_{ORC}$ ($/hr)	$\dot{C}_{ARC}$ ($/hr)	$\dot{C}_{VRC}$ ($/hr)	$\dot{C}_T$ ($/hr)
Pentane	47.61	26.7	9.51	0.72	84.53
Butane	47.61	26.61	8.884	0.694	83.81
R245fa	47.66	29.12	7.534	0.6081	84.93
MDM	47.68	27.8	18.47	1.471	95.43
Octane	47.61	26.01	9.326	0.7221	82.17

4.3.2. Effect of Inlet Temperatures of the ORT

Table 4.11 and Figure 4.2 present the work net ($\dot{W}_{net}$) results of the SCCHP system for various organic fluids and different inlet temperatures of the ORT. The results show that the work net of the SCCHP system reduces as the inlet temperatures of the ORT increase due to the decrease in the mass flow rate of the ORC fluid at high temperatures. The SCCHP system with R245fa as a working fluid has a high work

net at 120°C (198.9 kW), whereas the system with n-pentane has a low work net (158.8 kW). The findings demonstrate that as T_7 increases from 120°C to 165°C, $\dot{W}_{net}$ decreases from 198.9 kW to 55.43 kW for the SCCHP system with R245fa, while the $\dot{W}_{net}$ decreases from 158.8 kW to 27.04 kW for the SCCHP system with n-pentane.

Table 4.11. The work net results of the CCHP system for various organic fluids and different inlet temperatures of the ORT.

T7	Pentane	Butane	R245fa	MDM	Octane
120	158.8	185.1	198.9	162.5	186.5
125	141.1	164.2	177.2	140.5	170
130	124.3	145	157.7	119.8	154.2
135	108.3	127.3	139.9	100.4	139
140	93.15	110.8	123.4	81.98	124.3
145	78.7	95.25	108.1	64.6	110.3
150	64.92	80.64	93.77	48.14	96.79
155	51.74	66.82	80.27	32.54	83.77
160	39.13	53.72	67.52	17.72	71.24
165	27.04	41.26	55.43	3.636	59.16

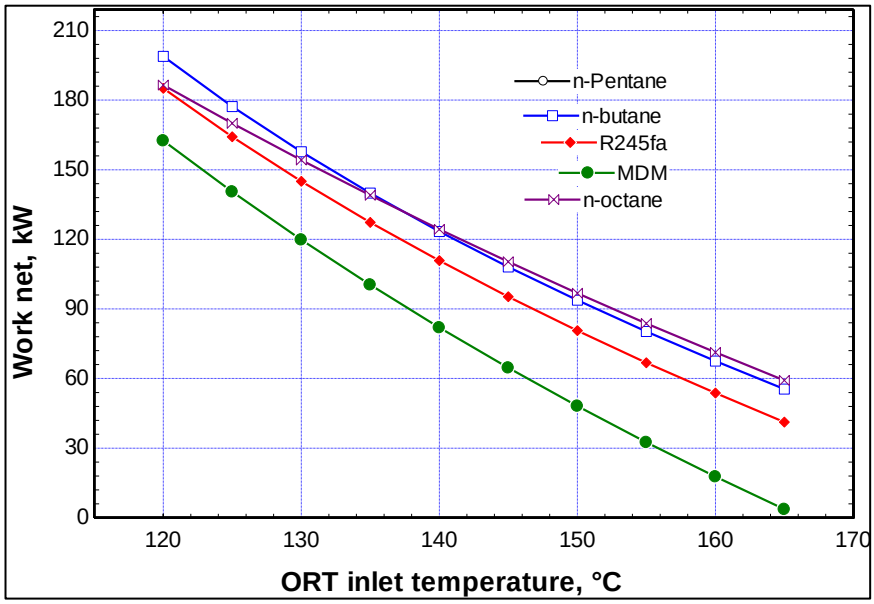

Figure 4.2. Impact of ORT inlet temperatures on the work output of the CCHP system.

For different organic fluids and varied intake temperatures of the ORT, the total cost $\dot{C}_T$ results of the SCCHP system are shown in Table 4.12 and Figure 4.3. The results show that the total cost rate of the SCCHP system increases with an increase in the inlet temperatures of the ORT.

Table 4.12. The total cost results of the CCHP system for various organic fluids and different inlet temperatures of the ORT.

T_7, (°C)	Pentane	Butane	R245fa	MDM	Octane
120	82.22	81.59	82.96	90.25	82.08
125	84.27	84.12	85.63	92.51	83.86
130	86.21	86.39	87.97	94.63	85.57
135	88.04	88.47	90.08	96.63	87.22
140	89.78	90.4	92	98.52	88.82
145	91.44	92.19	93.77	100.3	90.35
150	93.02	93.86	95.4	102	91.82
155	94.51	95.42	96.92	103.6	93.24
160	95.94	96.89	98.34	105	94.6
165	97.29	98.26	99.67	106.4	95.91

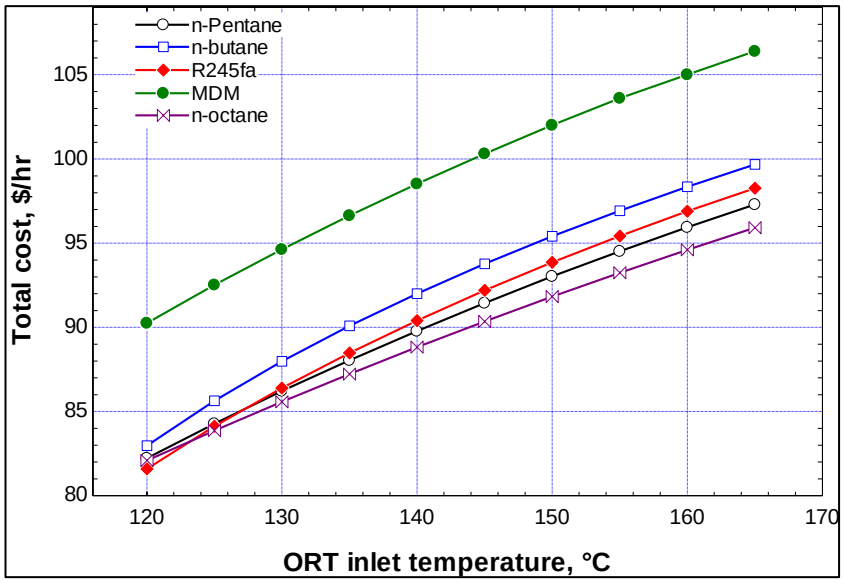

Figure 4.3. Impact of ORT inlet temperatures on the total cost of the CCHP system.

The SCCHP system utilizing MDM as the working fluid has a significantly higher overall cost at all temperatures at the input of ORT, unlike the system employing n-octane, demonstrating comparatively lower total cost. The results indicate that when the T_7 rises from 120°C to 165°C, the $\dot{C}_T$ increases from 92.51 $/hr to 106.4 $/hr for the SCCHP system with MDM, whereas the $\dot{C}_T$ rise from 83.67 $/hr to 94.6 $/hr for the SCCHP system with n-octane. It is also shown that the SCCHP with the n-butane has a lower cost rate at the minimum temperature at the inlet of ORT (about 81.59).

Table 4.13 and Figure 4.4 reveal the different thermal efficiency ($\eta_{th\,ermal}$) of the SCCHP system with various organic fluids and varying intake temperatures of the ORT. The findings indicate that the $\eta_{th\,ermal}$ of the SCCHP system diminishes as the inlet temperatures of the ORT rise, mostly because of the decline in net work at high temperatures at the ORT inlet.

Table 4.13. The thermal efficiency results of the CCHP system for various organic fluids and different inlet temperatures of the ORT.

T_7, (°C)	Pentane	Butane	R245fa	MDM	Octane
120	0.7657	0.7677	0.7741	0.7396	0.7644
125	0.7553	0.7544	0.7601	0.7289	0.7555
130	0.7455	0.7425	0.7478	0.7188	0.747
135	0.7363	0.7316	0.7367	0.7094	0.7389
140	0.7276	0.7216	0.7265	0.7004	0.7312
145	0.7193	0.7123	0.7173	0.692	0.7238
150	0.7115	0.7036	0.7087	0.6841	0.7166
155	0.7041	0.6955	0.7007	0.6766	0.7098
160	0.697	0.688	0.6932	0.6694	0.7032
165	0.6902	0.6808	0.6862	0.6627	0.6969

The SCCHP system utilizing R245fa as the working fluid has a much higher $\eta_{th\,ermal}$ of 77.41% at a temperature of 120°C, compared to the system employing MDM which achieves a lesser efficiency of 73.96%. The results indicate that when the temperature T_7 climbs from 120°C to 165°C, the $\eta_{th\,ermal}$ of the SCCHP system with R245fa reduces from 77.41% to 68.62%, while the $\eta_{th\,ermal}$ of the SCCHP system with MDM declines from 73.96% to 66.27%.

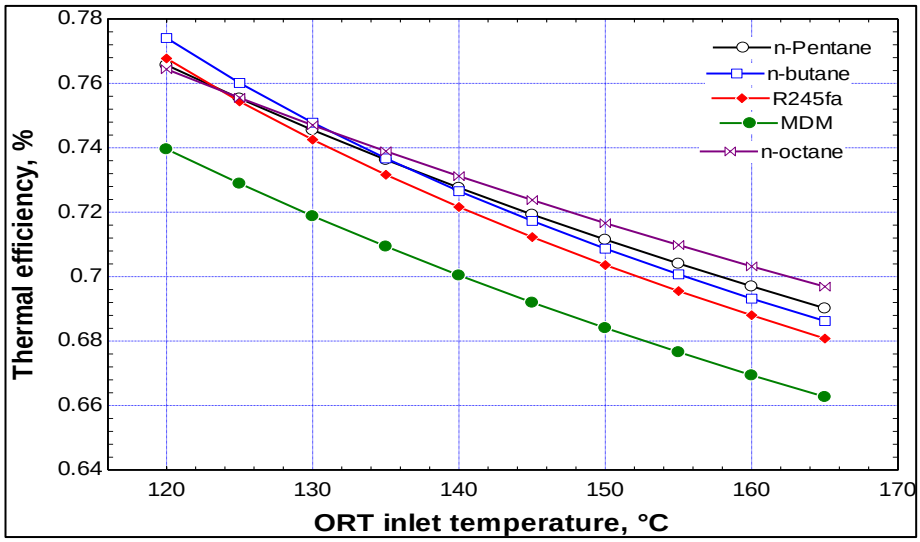

Figure 4.4. Impact of ORT inlet temperatures on the thermal efficiency of the CCHP system.

Table 4.14 and Figure 4.5 display the exergy efficiency (ψ_{exergy}) findings of the SCCHP system for different organic fluids and variable input temperatures of the ORT.

Table 4.14. The exergy efficiency results of the CCHP system for various organic fluids and different inlet temperatures of the ORT.

T_7, (°C)	Pentane	Butane	R245fa	MDM	Octane
120	0.1714	0.1693	0.1753	0.162	0.1742
125	0.1666	0.1638	0.1694	0.1568	0.17
130	0.1622	0.1588	0.1641	0.1518	0.1659
135	0.1579	0.1542	0.1594	0.1471	0.1621
140	0.1539	0.1499	0.155	0.1427	0.1583
145	0.1501	0.1459	0.1509	0.1386	0.1548
150	0.1465	0.1421	0.1472	0.1347	0.1514
155	0.143	0.1386	0.1437	0.1309	0.1481
160	0.1397	0.1353	0.1403	0.1274	0.1449
165	0.1366	0.1321	0.1372	0.1241	0.1418

The results show that the ψ_{exergy} curves of the SCCHP system are like the $\eta_{th\,ermal}$ curves, but the values are very small due to the huge exergy destruction by the solar

collectors. Based on the results, it is evident that at 120°C, the SCCHP system using R245fa as the working fluid achieves a much higher ψ_{exergy} (17.53%) than the MDM system (16.2%).

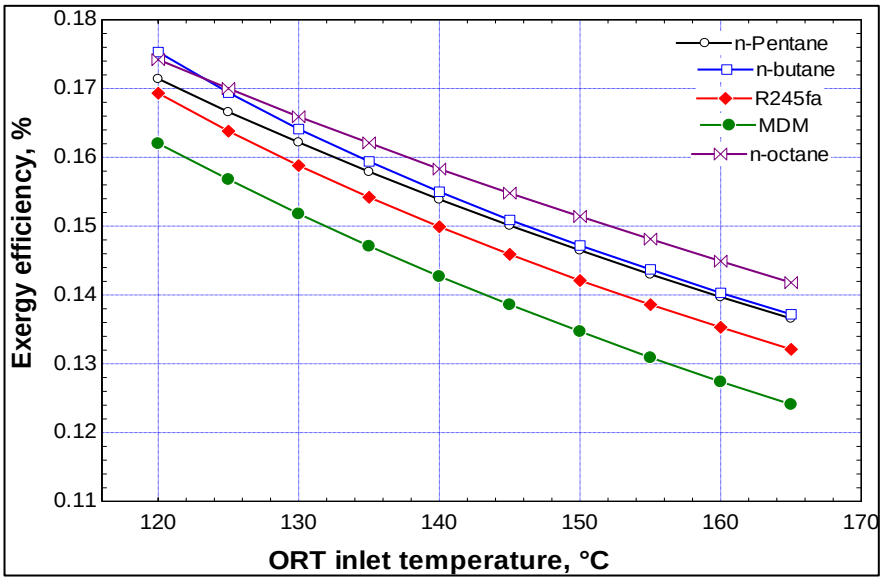

Figure 4.5. Impact of ORT inlet temperatures on the exergy efficiency of the CCHP system.

Table 4.15 and Figure 4.6 show the results of the SCCHP system's total exergy destruction for various organic fluids and ORT input temperatures. Because the heat transfer rate to the environment rises with increasing ORT input temperatures, the results demonstrate that the exergy destruction of the SCCHP system grows concerning these intake temperatures. The SCCHP system utilizing MDM as the working fluid has the highest exergy destruction at a temperature of 120°C, amounting to 5123 kW. In contrast, the system employing R245fa has the lowest exergy destruction, measuring 4830 kW.

Table 4.15. The total exergy destruction results of the CCHP system for various organic fluids and different inlet temperatures of the ORT.

T_7, (°C)	Pentane	Butane	R245fa	MDM	Octane
120	4926	4891	4830	5123	4913
125	5020	5009	4954	5223	4994
130	5107	5117	5064	5316	5071
135	5190	5214	5163	5405	5145
140	5269	5304	5254	5488	5216
145	5343	5388	5337	5566	5284
150	5413	5466	5414	5640	5349
155	5481	5539	5486	5711	5411
160	5545	5608	5553	5777	5472
165	5606	5673	5617	5840	5529

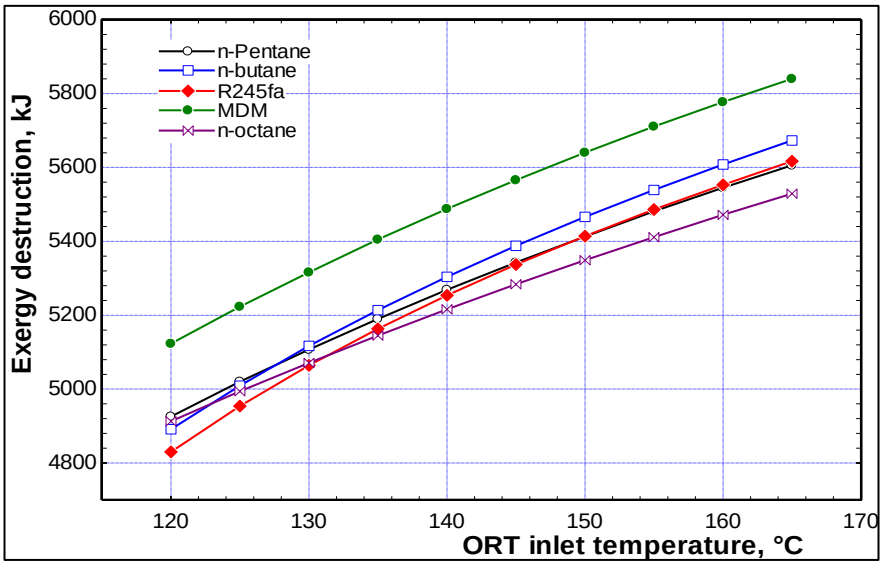

Figure 4.6. Impact of ORT inlet temperatures on the total exergy destruction of the CCHP system.

CHAPTER 5

CONCLUSION

This research study presents a suggested model for a solar combined cycle heat power (SCCHP) system, which integrates cooling, heating, and electricity generation. The system is designed to be suitable for government facilities, big hospitals, or residential complexes in Baghdad, Iraq. The type of collector is SPTC, and the optimum working fluid for the SCCHP system is n-octane. The system's continuous and stable operation is facilitated by the presence of a storage tank that stores the accumulated solar energy. 3E analysis is applied to the system (energy, exergy, and exergo-economic analysis). The SCCHP system generates 210 kW of electricity, 3965 kW of heat, and has a cooling load of 249.4 kW. It provides a water supply at a temperature of 80 °C, which is appropriate for residential usage. The system's thermal efficiency was determined to be 76.55%. Exergy analysis is conducted to accurately assess the extent of losses, identify their sources and locations, and estimate the actual efficiencies of the components. As a result of this study, the exergy efficiency of the SCCHP system is assessed to be 17.75%. The findings derived from the current investigation may be summarized as follows:

- The current system's energy efficiency is determined to be 76.55%. The SCCHP system achieves improved efficiency by generating process heat as a byproduct in addition to the cooling process.
- Solar collectors, ORC evaporators, and the ORC heat exchanger have the highest exergy destruction. The primary factor is the elevated heat transfer rates and temperature disparity shown by the working fluids.
- The exergo-economic factor of the SCCHP system was determined to be 63.32%, indicating that the proportion of expenses attributed to exergy destruction is less than the system's initial capital investment cost.

- The solar collector and ORC evaporator hold the highest significance from an exergo-economic perspective since its $\dot{C}_T$ value surpasses other components.
- An investigation is conducted to examine the impact of the Organic Rankine Cycle (ORC) working fluid on the functioning of the system. Out of the five chosen working fluids in this investigation, n-octane is the best suitable choice since it has the maximum capacity to produce work and a lower cost rate. Nevertheless, after examining the outcomes of energy and exergy efficiency, as well as analyzing the rates of total exergy destruction, it becomes evident that utilizing R245fa as a working fluid is the most suitable choice.
- An analysis of the impact of ORT intake temperature on SCCHP system operation and performance demonstrates that raising the ORT inlet temperature results in a drop in work net, an increase in total cost rate, and, therefore, a reduction in the thermal and exergy efficiencies of the system.

REFERENCES

1. Liu, M., Shi, Y., and Fang, F., "Combined cooling, heating and power systems: A survey", ***Renewable And Sustainable Energy Reviews***, 35: 1–22 (2014).

2. Song, Y.-J., Li, B., Zhang, C.-Y., Wang, W.-W., Zhao, F.-Y., and Guo, J.-H., "Solar Photo-Voltaic and thermal (PVT) system facilitated with novel coaxial condensing heat pipe (CCHP): Thermo hydrodynamic modelling and parametric optimization for overall operation performance", ***Solar Energy***, 264: 112019 (2023).

3. Liu, Y., Han, J., and You, H., "Exergoeconomic analysis and multi-objective optimization of a CCHP system based on SOFC/GT and transcritical CO2 power/refrigeration cycles", ***Applied Thermal Engineering***, 230: 120686 (2023).

4. Zhang, N., Wang, Z., and Han, W., "Analysis of A Solar Assisted Combined Cooling, Heating and Power (SCCHP) System", ***Energy Procedia***, 142: 55–62 (2017).

5. Wang, J., Han, Z., and Guan, Z., "Hybrid solar-assisted combined cooling, heating, and power systems: A review", ***Renewable And Sustainable Energy Reviews***, 133: 110256 (2020).

6. Romero, M., "Solar thermal CSP technology", ***Energ And Environment***, 3 (February 2014): (2020).

7. Nawaf, M. Y., Akroot, A., and Wahhab, H. A. A., "NUMERICAL SIMULATION OF A POROUS MEDIA SOLAR COLLECTOR INTEGRATED WITH THERMAL ENERGY STORAGE SYSTEM", (2023).

8. Oliveira, A. C., Afonso, C., Matos, J., Riffat, S., Nguyen, M., and Doherty, P., "A combined heat and power system for buildings driven by solar energy and gas", ***Applied Thermal Engineering***, 22 (6): 587–593 (2002).

9. Lima, A. A. S., Leite, G. de N. P., Ochoa, A. A. V., Dos Santos, C. A. C., da Costa, J. A. P., Michima, P. S. A., and Caldas, A. M. A., "Absorption refrigeration systems based on ammonia as refrigerant using different absorbents: Review and applications", ***Energies***, 14 (1): (2021).

10. Aghaziarati, Z. and Aghdam, A. H., "Thermoeconomic analysis of a novel combined cooling, heating and power system based on solar organic Rankine cycle and cascade refrigeration cycle", ***Renewable Energy***, 164: 1267–1283 (2021).

11. Yang, K., Zhu, N., Ding, Y., Chang, C., Wang, D., and Yuan, T., "Exergy and exergoeconomic analyses of a combined cooling, heating, and power (CCHP) system based on dual-fuel of biomass and natural gas", ***Journal Of Cleaner Production***, 206: 893–906 (2019).

12. Aghaziarati, Z. and Aghdam, A. H., "Thermoeconomic analysis of a novel combined cooling, heating and power system based on solar organic Rankine cycle and cascade refrigeration cycle", ***Renewable Energy***, 164: 1267–1283 (2021).

13. Wu, D. W. and Wang, R. Z., "Combined cooling, heating and power: A review", ***Progress In Energy And Combustion Science***, 32 (5–6): 459–495 (2006).

14. Wang, J., Lu, Y., Yang, Y., and Mao, T., "Thermodynamic performance analysis and optimization of a solar-assisted combined cooling, heating and power system", ***Energy***, 115: 49–59 (2016).

15. Abdullah-Al-Mahbub, M., Islam, A. R. M. T., Almohamad, H., Al Dughairi, A. A., Al-Mutiry, M., and Abdo, H. G., "Different Forms of Solar Energy Progress: The Fast-Growing Eco-Friendly Energy Source in Bangladesh for a Sustainable Future", ***Energies***, 15 (18): (2022).

16. Dawood, T. A., Raphael, R., Barwari, I., and Akroot, A., "Solar Energy and Factors Affecting the Efficiency and Performance of Panels in Erbil / Kurdistan", ***International Journal Of Heat And Technology***, 41 (2): 304–312 (2023).

17. Khalil, A., Rajab, Z., Amhammed, M., and Asheibi, A., "The benefits of the transition from fossil fuel to solar energy in Libya: A street lighting system case study", ***Applied Solar Energy (English Translation Of Geliotekhnika)***, 53 (2): 138–151 (2017).

18. Khudhur, J., Akroot, A., and Al-samari, A., "Experimental Investigation of Direct Solar Photovoltaics that Drives Absorption Refrigeration System", ***Journal Of Advanced Research In Fluid Mechanics And Thermal Sciences***, 1 (1): 116–135 (2023).

19. Saffaripour, M. H., Mehrabian, M. A., and Bazargan, H., "Predicting solar radiation fluxes for solar energy system applications", ***International Journal Of Environmental Science And Technology***, 10 (4): 761–768 (2013).

20. Li, Q., Shirazi, A., Zheng, C., Rosengarten, G., Scott, J. A., and Taylor, R. A., "Energy concentration limits in solar thermal heating applications", ***Energy***, 96: 253–267 (2016).

21. Kumar, L., Hasanuzzaman, M., and Rahim, N. A., "Global advancement of solar thermal energy technologies for industrial process heat and its future prospects: A review", ***Energy Conversion And Management***, 195 (May): 885–908 (2019).

22. Bdaiwi, M., Akroot, A., Wahhab, H. A. A., and Mahariq, I., "NUMERICAL ANALYSIS OF THE STEAM TURBINE PERFORMANCE IN POWER STATION WITH A LOW POWER CYCLE", (2023).

23. Peterseim, J. H., Tadros, A., Hellwig, U., and White, S., "Increasing the efficiency of parabolic trough plants using thermal oil through external superheating with biomass", ***Energy Conversion And Management***, 77: 784–793 (2014).

24. Kalogirou, S. A., "Solar Thermal Collectors and Applications", Progress in Energy and Combustion Science, 231–295 (2004).

25. Pili, R., Spliethoff, H., and Wieland, C., "Dynamic simulation of an Organic Rankine Cycle - Detailed model of a kettle boiler", ***Energies***, 10 (4): (2017).

26. BademliOğlu, A. H., Canbolat, A. S., Yamankaradeniz, N., and Kaynakli, Ö., "A parametric analysis of the performance of organic rankine cycle with heat recovery exchanger and its statistical evaluation", ***Isi Bilimi Ve Teknigi Dergisi/ Journal Of Thermal Science And Technology***, 39 (2): 121–135 (2019).

27. Kareem, A. F., Akroot, A., Abdul Wahhab, H. A., Talal, W., Ghazal, R. M., and Alfaris, A., "Exergo–Economic and Parametric Analysis of Waste Heat Recovery from Taji Gas Turbines Power Plant Using Rankine Cycle and Organic Rankine Cycle", ***Sustainability (Switzerland)***, 15 (12): (2023).

28. Mithat Delibaş, H., Kayabaşı, E., Mithat Delibas, H., and Kayabasi, E., "Environment and Economy Assessment of Waste Heat Recovery Technologies in Marine Industry", ***The International Journal Of Materials And Engineering Technology***, 004 (2): 133–146 (2021).

29. Baral, S., Kim, D., Yun, E., and Kim, K. C., "Experimental and thermoeconomic analysis of small-scale solar organic rankine cycle (SORC) system", ***Entropy***, 17 (4): 2039–2061 (2015).

30. Baral, S., Kim, D., Yun, E., and Kim, K. C., "Experimental and thermoeconomic analysis of small-scale solar organic rankine cycle (SORC) system", ***Entropy***, 17 (4): 2039–2061 (2015).

31. Salem, M., Fahim Alavi, M., Mahariq, I., Accouche, O., and El Haj Assad, M., "Applications of Thermal Energy Storage in Solar Organic Rankine Cycles: A Comprehensive Review", ***Frontiers In Energy Research***, 9 (October): 1–11 (2021).

32. Gupta, P. R., Tiwari, A. K., and Said, Z., "Solar organic Rankine cycle and its poly-generation applications – A review", ***Sustainable Energy Technologies And Assessments***, 49 (July 2021): 101732 (2022).

33. Salem, M., Fahim Alavi, M., Mahariq, I., Accouche, O., and El Haj Assad, M., "Applications of Thermal Energy Storage in Solar Organic Rankine Cycles: A

Comprehensive Review", ***Frontiers In Energy Research***, 9 (October): 1–11 (2021).

34. Gupta, P. R., Tiwari, A. K., and Said, Z., "Solar organic Rankine cycle and its poly-generation applications – A review", ***Sustainable Energy Technologies And Assessments***, 49 (July 2021): 101732 (2022).

35. Herrera-Romero, J. and Colorado-Garrido, D., "Comparative Study of a Compression–Absorption Cascade System Operating with NH3-LiNO3, NH3-NaSCN, NH3-H2O, and R134a asWorking Fluids", ***Processes***, 8 (7): 816 (2020).

36. Saleh, B., Aly, A. A., Alsehli, M., Elfasakhany, A., and Bassuoni, M. M., "Performance analysis and working fluid selection for single and two stages vapor compression refrigeration cycles", ***Processes***, 8 (9): (2020).

37. Herrera-Romero, J. and Colorado-Garrido, D., "Comparative Study of a Compression–Absorption Cascade System Operating with NH3-LiNO3, NH3-NaSCN, NH3-H2O, and R134a asWorking Fluids", ***Processes***, 8 (7): 816 (2020).

38. Kasi, P. and Cheralathan, M., "Review of cascade refrigeration systems for vaccine storage", ***Journal Of Physics: Conference Series***, 2054 (1): (2021).

39. Turgut, M. S. and Turgut, O. E., "Comparative investigation and multi objective design optimization of a cascaded vapor compression absorption refrigeration system operating with different refrigerants in the vapor compression cycle", ***Heat And Mass Transfer/Waerme- Und Stoffuebertragung***, 55 (2): 467–488 (2019).

40. Sarbu, I. and Sebarchievici, C., "A comprehensive review of thermal energy storage", ***Sustainability (Switzerland)***, 10 (1): (2018).

41. Alva, G., Lin, Y., and Fang, G., "An overview of thermal energy storage systems", ***Energy***, 144: 341–378 (2018).

42. Hou, H., Wu, J., Ding, Z., Yang, B., and Hu, E., "Performance analysis of a solar-assisted combined cooling, heating and power system with an improved operation strategy", ***Energy***, 227: 120516 (2021).

43. Zhang, L., Li, F., Sun, B., and Zhang, C., "Integrated optimization design of combined cooling, heating, and power system coupled with solar and biomass energy", ***Energies***, 12 (4): (2019).

44. Chen, Y., Xu, D., Chen, Z., Gao, X., and Han, W., "Energetic and exergetic analysis of a solar-assisted combined power and cooling (SCPC) system with two different cooling temperature levels", ***Energy Conversion And Management***, 182 (August 2018): 497–507 (2019).

45. Ravindra, V. and Ramgopal, M., "Thermodynamic Analysis of a Solar Assisted Combined Cooling, Heating and Power System with Different Cooling Cycle Configurations", ***INAE Letters***, 3 (2): 107–113 (2018).

46. Salimi, M., Hosseinpour, M., Mansouri, S., and Borhani, T. N., "Environmental Aspects of the Combined Cooling, Heating, and Power (CCHP) Systems: A Review", ***Processes***, 10 (4): 1–23 (2022).

47. Tonekaboni, N., Feizbahr, M., Tonekaboni, N., Jiang, G. J., and Chen, H. X., "Optimization of Solar CCHP Systems with Collector Enhanced by Porous Media and Nanofluid", ***Mathematical Problems In Engineering***, 2021: (2021).

48. Wang, S. and Fu, Z., "Thermodynamic and economic analysis of solar assisted CCHP-ORC system with DME as fuel", ***Energy Conversion And Management***, 186 (December 2018): 535–545 (2019).

49. Assareh, E., Dejdar, A., Ershadi, A., Jafarian, M., Mansouri, M., Salek roshani, A., Azish, E., Saedpanah, E., Aghajari, M., and Wang, X., "Performance analysis of solar-assisted-geothermal combined cooling, heating, and power (CCHP) systems incorporated with a hydrogen generation subsystem", ***Journal Of Building Engineering***, 65 (September 2022): 105727 (2023).

50. Heydari, A. and Sadati, S. E., "The effect of materials used in office building envelope on the capacity and performance of a solar-assisted cooling heating and power system", ***Environmental Progress And Sustainable Energy***, 42 (6): 1–18 (2023).

51. Wang, J., Li, S., Zhang, G., and Yang, Y., "Performance investigation of a solar-assisted hybrid combined cooling, heating and power system based on energy, exergy, exergo-economic and exergo-environmental analyses", ***Energy Conversion And Management***, 196 (June): 227–241 (2019).

52. Han, Z., Wang, J., Cui, Z., Lu, C., and Qi, X., "Multi-objective optimization and exergoeconomic analysis for a novel full-spectrum solar-assisted methanol combined cooling, heating, and power system", ***Energy***, 237: 121537 (2021).

53. Wang, J., Lu, Y., Yang, Y., and Mao, T., "Thermodynamic performance analysis and optimization of a solar-assisted combined cooling, heating and power system", ***Energy***, 115: 49–59 (2016).

54. Wang, J., Chen, Y., and Lior, N., "Exergo-economic analysis method and optimization of a novel photovoltaic/thermal solar-assisted hybrid combined cooling, heating and power system", ***Energy Conversion And Management***, 199 (June): 111945 (2019).

55. Chen, E., Xie, M., Jia, T., Zhao, Y., and Dai, Y., "Performance assessment of a solar-assisted absorption-compression system for both heating and cooling", ***Applied Energy***, 328 (May): 120238 (2022).

56. Chen, E., Zhao, Y., Wang, M., Bian, M., Cai, W., Li, B., and Dai, Y., "Experimental investigation of a solar-assisted absorption-compression system for heating and cooling", ***Solar Energy***, 257 (February): 18–33 (2023).

57. Tan, L., Chen, C., Gong, Z., and Xia, L., "Performance evaluation on a novel combined cool/heat and power (CCP/CHP) system integrating an SOFC-GT plant with a solar-assisted LiBr absorption cooling/heating unit", ***Energy***, 283 (May): 129102 (2023).

58. Su, B., Han, W., Zhang, X., Chen, Y., Wang, Z., and Jin, H., "Assessment of a combined cooling, heating and power system by synthetic use of biogas and solar energy", ***Applied Energy***, 229 (May): 922–935 (2018).

59. Wang, J. and Yang, Y., "Energy, exergy and environmental analysis of a hybrid combined cooling heating and power system utilizing biomass and solar energy", ***Energy Conversion And Management***, 124: 566–577 (2016).

60. Bahria, S., Amirat, M., Hamidat, A., El Ganaoui, M., and Slimani, M., "Parametric study of solar heating and cooling systems in different climates of Algeria – A comparison between conventional and high-energy-performance buildings", ***Energy***, 113: 521–535 (2016).

61. Cengel, Y. A. and Boles, M. A., "Thermodynamics: An Engineering Approach 8th Edition", McGraw-Hill, (2015).

62. MORAN, M. J. and SHAPIRO, HOWARD N.BOETTNER, D. D. M. B. B., "Fundamentals of Engineering Thermodynamics", WILEY, 14–61 (2020).

63. Xi, Z., Eshaghi, S., and Sardari, F., "Energy, exergy, and exergoeconomic analysis of a polygeneration system driven by solar energy with a thermal energy storage tank for power, heating, and freshwater production", ***Journal Of Energy Storage***, 36 (September 2020): 102429 (2021).

64. Akroot, A. and Namli, L., "Performance assessment of an electrolyte-supported and anode-supported planar solid oxide fuel cells hybrid system", ***J Ther Eng***, 7 (7): 1921–1935 (2021).

65. Khoshgoftar Manesh, M. H., Mousavi Rabeti, S. A., Nourpour, M., and Said, Z., "Energy, exergy, exergoeconomic, and exergoenvironmental analysis of an innovative solar-geothermal-gas driven polygeneration system for combined power, hydrogen, hot water, and freshwater production", ***Sustainable Energy Technologies And Assessments***, 51 (April 2021): (2022).

66. Yilmaz, F., Ozturk, M., and Selbas, R., "Thermodynamic investigation of a concentrating solar collector based combined plant for poly-generation", ***International Journal Of Hydrogen Energy***, 45 (49): 26138–26155 (2020).

67. Anvari, S., Mahian, O., Taghavifar, H., Wongwises, S., and Desideri, U., "4E analysis of a modified multigeneration system designed for power,

heating/cooling, and water desalination", ***Applied Energy***, 270 (February): 115107 (2020).

68. Alsunousi, M. and Kayabasi, E., "Techno-economic assessment of a floating photovoltaic power plant assisted methanol production by hydrogenation of CO2 captured from Zawiya oil refinery", ***International Journal Of Hydrogen Energy***, 57: 589–600 (2024).

69. Akroot, A., "Effect of Operating Temperatures on the Performance of a SOFCGT Hybrid System", ***International Journal Of Trend In Scientific Research And Development***, Volume-3 (Issue-3): 1512–1515 (2019).

70. Anvari, S., Mahian, O., Taghavifar, H., Wongwises, S., and Desideri, U., "4E analysis of a modified multigeneration system designed for power, heating/cooling, and water desalination", ***Applied Energy***, 270 (February): 115107 (2020).

71. Akroot, A. and Nadeesh, A., "Performance Analysis of Hybrid Solid Oxide Fuel Cell-Gas Turbine Power System", (2021).

72. Bellos, E., Lykas, P., Sammoutos, C., Kitsopoulou, A., Korres, D., and Tzivanidis, C., "Thermodynamic investigation of a solar-driven organic Rankine cycle with partial evaporation", ***Energy Nexus***, 11 (July): 100229 (2023).

73. Ozturk, M. and Dincer, I., "Thermodynamic analysis of a solar-based multi-generation system with hydrogen production", ***Applied Thermal Engineering***, 51 (1–2): 1235–1244 (2013).

74. Ozturk, M. and Dincer, I., "Thermodynamic analysis of a solar-based multi-generation system with hydrogen production", ***Applied Thermal Engineering***, 51 (1–2): 1235–1244 (2013).

75. Wang, J., Lu, Z., Li, M., Lior, N., and Li, W., "Energy, exergy, exergoeconomic and environmental (4E) analysis of a distributed generation solar-assisted CCHP (combined cooling, heating and power) gas turbine system", ***Energy***, 175: 1246–1258 (2019).

76. Talal, W. and Akroot, A., "An Exergoeconomic Evaluation of an Innovative Polygeneration System Using a Solar-Driven Rankine Cycle Integrated with the Al-Qayyara Gas Turbine Power Plant and the Absorption Refrigeration Cycle", ***Machines***, 12 (2): 133 (2024).

77. Fan, R. and Xi, H., "Exergoeconomic optimization and working fluid comparison of low-temperature Carnot battery systems for energy storage", ***Journal Of Energy Storage***, 51 (March): 104453 (2022).

78. Xi, Z., Eshaghi, S., and Sardari, F., "Energy, exergy, and exergoeconomic analysis of a polygeneration system driven by solar energy with a thermal

energy storage tank for power, heating, and freshwater production", ***Journal Of Energy Storage***, 36 (September 2020): 102429 (2021).

79. Elmorsy, L., Morosuk, T., and Tsatsaronis, G., "Exergy-based analysis and optimization of an integrated solar combined-cycle power plant", ***Entropy***, 22 (6): 1–20 (2020).

80. Xie, N., Xiao, Z., Du, W., Deng, C., Liu, Z., and Yang, S., "Thermodynamic and exergoeconomic analysis of a proton exchange membrane fuel cell/absorption chiller CCHP system based on biomass gasification", ***Energy***, 262 (PB): 125595 (2023).

81. Dhahad, H. A., Ahmadi, S., Dahari, M., Ghaebi, H., and Parikhani, T., "Energy, exergy, and exergoeconomic evaluation of a novel CCP system based on a solid oxide fuel cell integrated with absorption and ejector refrigeration cycles", ***Thermal Science And Engineering Progress***, 21 (May 2020): 100755 (2021).

82. Akrami, E., Nemati, A., Nami, H., and Ranjbar, F., "Exergy and exergoeconomic assessment of hydrogen and cooling production from concentrated PVT equipped with PEM electrolyzer and LiBr-H2O absorption chiller", ***International Journal Of Hydrogen Energy***, 43 (2): 622–633 (2018).

83. Talal, W. and Akroot, A., "Exergoeconomic Analysis of an Integrated Solar Combined Cycle in the Al-Qayara Power Plant in Iraq", ***Processes***, 11 (3): (2023).

84. Besevli, B., Kayabasi, E., Akroot, A., Talal, W., Alfaris, A., Assaf, Y. H., Nawaf, M. Y., Bdaiwi, M., and Khudhur, J., "Technoeconomic Analysis of Oxygen-Supported Combined Systems for Recovering Waste Heat in an Iron-Steel Facility", ***Applied Sciences***, 14 (6): 2563 (2024).

85. Patel, B., Desai, N. B., and Kachhwaha, S. S., "Optimization of waste heat based organic Rankine cycle powered cascaded vapor compression-absorption refrigeration system", ***Energy Conversion And Management***, 154 (July): 576–590 (2017).

86. Jang, Y. and Lee, J., "Optimizations of the organic Rankine cycle-based domestic CHP using biomass fuel", ***Energy Conversion And Management***, 160 (January): 31–47 (2018).

RESUME

His name is Shawqi Hussein Krain AL- GAWWAM. His primary and elementary education in Iraq. He is a mechanical engineer who graduated from the Faculty of Engineering, University of Baghdad – Iraq. He received his bachelor's degree in 1998. He currently works as an employee in the Ministry of Science and Technology. He is currently studying for his master's degree at Karabük University in the field of Mechanical Engineering.